Best
Available
Copy

AD-A009 422

EFFECTS OF HIGH POWER LASERS, NUMBER 5

Stuart G. Hibben, et al

Informatics, Incorporated

Prepared for:

Navy Foreign Language Service
Defense Advanced Research Projects Agency

1 May 1975

DISTRIBUTED BY:

NTIS

National Technical Information Service
U. S. DEPARTMENT OF COMMERCE

UNCLASSIFIED

SECURITY CLASSIFICATION OF THIS PAGE (When Data Entered)

AD-A009 422

REPORT DOCUMENTATION PAGE

READ INSTRUCTIONS BEFORE COMPLETING FORM

1. REPORT NUMBER	2. GOVT ACCESSION NO.
3. RECIPIENT'S CATALOG NUMBER	Scientific . . . Interim
4. TITLE (and Subtitle)	Effects of High Power Lasers, No. 5 September, 1974 - February, 1975
5. TYPE OF REPORT & PERIOD COVERED	
6. PERFORMING ORG. REPORT NUMBER	
7. AUTHOR(s)	S. G. Hibben, J. Kourilo, M. Ness, B. Shresta
8. CONTRACT OR GRANT NUMBER(s)	N00600-75-C-0018
9. PERFORMING ORGANIZATION NAME AND ADDRESS	Informatics Inc. 6000 Executive Boulevard Rockville, Maryland 20852
10. PROGRAM ELEMENT, PROJECT, TASK AREA & WORK UNIT NUMBERS	DARPA Order No. 2790 Program Code No. L13003
11. CONTROLLING OFFICE NAME AND ADDRESS	Defense Advance Research Projects Agency/TAO 1400 Wilson Boulevard Arlington, Virginia 22209
12. REPORT DATE	May 1, 1975
13. NUMBER OF PAGES	103
14. MONITORING AGENCY NAME & ADDRESS (if different from Controlling Office)	U. S. Navy Foreign Language Service 4301 Suitland Road, Bldg. 5 Washington, D. C. 20390
15. SECURITY CLASS. (of this report)	UNCLASSIFIED
15a. DECLASSIFICATION DOWNGRADING SCHEDULE	

16. DISTRIBUTION STATEMENT (of this Report)

Approved for public release; distribution unlimited.

17. DISTRIBUTION STATEMENT (of the abstract entered in Block 20, if different from Report)

18. SUPPLEMENTARY NOTES

Scientific . . . Interim

19. KEY WORDS (Continue on reverse side if necessary and identify by block number)

High power lasers
Beam-target interaction
Laser damage
Optical breakdown
Laser-plasma interaction

20. ABSTRACT (Continue on reverse side if necessary and identify by block number)

This is the fifth compilation of abstracts of Soviet studies on high power laser technology, covering material published from September 1974 through February 1975. Articles are grouped by laser interaction with metals, dielectrics, semiconductors, miscellaneous targets, and laser-plasma interaction.

DD FORM 1 JAN 73 1473 EDITION OF 1 NOV 65 IS OBSOLETE

UNCLASSIFIED

SECURITY CLASSIFICATION OF THIS PAGE (When Data Entered)

EFFECTS OF HIGH POWER LASERS, NO. 5

September 1974 - February 1975

Sponsored by

Defense Advanced Research Projects Agency

DARPA Order No. 2790

ARPA Order No. 2790
Program Code No. L13003
Name of Contractor:
Informatics Inc.
Effective Date of Contract:
July 1, 1974
Contract Expiration Date:
June 30, 1975
Amount of Contract: $306, 023

Contract No. N00600-75-C-0018
Principal Investigator:
Stuart G. Hibben
Tel: (301) 770-3000
Program Manager:
Klaus Liebhold
Tel: (301) 770-3000
Short Title of Work:
"Laser Effects"

This research was supported by the Defense Advanced Research Projects Agency and was monitored by the U. S. Navy Foreign Language Service under Contract No. N00600-75-C-0018. The publication of this report does not constitute approval by any government organization or Informatics Inc. of the inferences, findings, and conclusions contained herein. It is published solely for the exchange and stimulation of ideas.

informatics inc
Systems and Services Company
6000 Executive Boulevard
Rockville Maryland 20852
(301) 770-3000 Telex 89-521

1a

INTRODUCTION

This is the fifth compilation of abstracts of Soviet studies on high power laser technology, covering material published from September 1974 through February 1975. Articles are grouped by laser interaction with metals, dielectrics, semiconductors, miscellaneous targets, and laser-plasma interaction.

A first-author index and an index of source abbreviations are appended.

TABLE OF CONTENTS

1. Metal Targets 1
2. Dielectric Targets 18
3. Semiconductor Targets 40
4. Miscellaneous Studies 43
5. Laser-Plasma Interaction. 52
6. List of Source Abbreviations 92
7. Author Index to Abstracts 98

1. Metal Targets

Rykalin, N. N., A. A. Uglov, I. P. Dobrovol'skiy, and M. M. Nizametdinov. Action of laser radiation on metals at high ambient pressures. Kvantovaya elektronika, no. 9, 1974, 1928-1933.

Beam-target studies under ambient pressures up to 140 atm are reported. Laser bombardment of metals was conducted in a pressure chamber filled with nitrogen, and high-speed photographes were taken of the damage processes (Fig. 1). The radiation source was a free-running Nd laser with pulse duration τ_i = 0.5 millisec and energy from 1-10 joules. Metal specimens used were molybdenum and stainless steel of a few millimeters thickness.

Fig. 1. Photos of laser radiation interaction zone on a stainless steel plate of 2 mm thickness at (a) p = 110 atm.; (b) p = 70 atm.; (c) p = 30 atm.

At incident flux densities of 10^6 w/cm^2 and pressures below 50 atm, the interaction process in steel was followed by formation of a through hole, and the peripheral surface around the hole was covered with a crystallized phase. The volume of metal ejecta from the interaction zone decreased with increase of pressure above 50 atm, such that at pressures

in the range of 100-110 atm, neither craters nor fusion zones were found on the surface of the metal (Fig. 1).

The observed phenomena indicate that with an increase of ambient pressure, a combined effect occurs causing a reduction in material ejection and a change in the character of the interaction processes. This sharp reduction in ejecta with increase of ambient pressure is evidently caused by a decrease of incident radiation flux density due to shielding of the interaction surface during optical breakdown, which leads to a sharp decrease in transparency of the medium. High-speed photographs show formation of plasma clouds at pressures over 70 atm, which move counter to the laser beam with velocities on the order of 10 m/sec, and form a strong radiation shield. A possible mechanism is analyzed for this phenomenon, and it is shown that the optical shielding gets stronger with rise in plasma temperature.

Uglov, A. A. <u>Thermophysical and hydrodynamic phenomena in laser processing of metals.</u> FiKhOM, no. 5, 1974, 3-13.

Thermal and hydrodynamic problems in laser processing of metals are considered. The destruction mechanism is discussed of metals by a focused beam of variable flux density incident on the metal surface. A series of problems are outlined, solutions of which are vital to further progress in understanding processes in laser technology.

The article is presented in a general form, dealing with the following topics:

1. Thermophysical problems during radiation interaction.
2. Characteristics of laser interaction at:
   a) low flux density
   b) moderate flux density
   c) high flux density
3. Hydrodynamic and thermophysical processes.
4. Methods of analysis.

The author notes that thermophysical and hydrodynamic processes are in most cases the determining factors in processing with a focused laser beam. Despite a large number of theoretical and experimental works, it cannot be stated that the theoretical principles of this branch of laser technology have been definitively set down. Quantitative concepts of the resulting processes have been developed in regions of low flux density but only partly for moderate q and above. The main trend of studies at low q is the analysis of nonlinear problems of thermal conductivity, taking into account the temperature dependence of thermophysical coefficients. Stefan's problem is of significant interest for a two-phase medium and for analysing fusion movements.

Moving up to a q on the order of 10^5-10^6 w/cm^2 involves construction of a model for deep fusion, allowing for not only thermal but also hydrodynamic phenomena. For radiation interaction at moderate q, the problem still remains to determine a physical model for material destruction which takes into account phenomena in the layer of liquid phase adjoining the interaction surface. Model problems which account for the two-phase characteristics of a medium during material destruction, and the interaction of plasma formations with condensed phase and incident radiation at moderate and high flux densities, are of great importance. In general more rigorous theoretical and experimental work remains to be done in this field.

Dimitrov, G., and A. Petrakiyev. Investigating excitation conditions of luminescence spectra and spectral microanalysis using a neodymium laser in an atmosphere of air, oxygen, nitrogen and argon at 1 atm. Godishn. Sofiysk. un-t. Fiz. fak., no. 64-65, 1970-1972(1973), 531-552. (RZhF, 8/74, #8D1342). (Translation)

Evaporation processes and excitation of spectra were investigated during laser spectral microanalysis of metals and alloys in

atmospheres of air, oxygen, nitrogen or argon. As compared to measurements in air, in oxygen or argon a sharp increase in intensity of spectral lines at the noise level and the disappearance of the molecular cyanogen band were observed. Calibration curves are given for analysing low-alloy steels and silumin.

Yarema, S. Ya., M. I. Moysa, Z. M. Manyuk, I. B. Polutranko, and G. V. Plyatsko. Using laser radiation for facilitating crack formation in plates. FKhMM, no. 2, 1974, 54-57.

A standard method for testing crack resistance of materials is to use specimens with initially induced cracks in them. For this purpose initial cuts or notches are made in the specimens and cyclic loading is applied up to a point when through cracks appear. The present work studies the possibility of a significant lowering of the required cyclic loading, by using a laser beam on the apex of the initial cuts in thin plates.

Experiments were conducted with disc specimens of 230 mm diameter, thickness 4 mm made of hot-rolled 65G steel. Irradiation was by a neodymium laser with energy = 140 joules, pulse duration = 7 msec or with energy = 120 joules, pulse duration = 4 msec. A detailed description is included on the experimental procedure. Specimens were subjected to variable tensile loads up to 2400 kg and up to 10^6 cycles. It was seen that for a given elapsed time the force required for crack formation in specimens subjected to laser treatment was significantly less. The authors conclude that the present work confirms the advantage of using lasers to lower the required loadings and time consumption in inducing initial cracks in specimens.

Burenkov, G. L., V. B. Deymontovich, L. O. Zhenni-Mayskaya, M. Z. Kol'chinskiy, A. V. Perepelkin, and A. I. Raychenko. Structural and concentration changes in alloys subjected to laser radiation. Metallofizika, no. 45, 1973, 75-81.

Structural and concentration changes in Al-Si, Al-Cu and Al-Ni alloys were experimentally investigated in stable and unstable states after exposure to concentrated laser radiation. Ground and polished specimen surfaces were subjected to a ruby laser beam of moderate flux density ($\sim 10^6$ w/cm^2) and operating free-running at a nominal pulse width of 1 millisecond. Results are summarized as follows:

1). Structural Changes

Metallographic studies showed changes in microstructures in some layers adjacent to the inside surface of craters, formed during laser irradiation. The thickness of these layers increased in the direction from crater bottom to the surface hole, depending on the properties of the irradiated alloys, its value did not exceed a few microns.

Microphotographs of a Al-Cu alloy system in stable and unstable states are shown in Fig. 1. Three distinct zones are seen in the crater region: (a) molten metal zone; (b) dislocation zone and (c) zone with broken grains. Craters formed in specimens in an unstable state were approximately two times deeper than in those in the stable state. In the case of Al-Si and Al-Ni alloy systems, this differences was not detected. Table 1 gives the values of depth and diameters of craters in the tested alloys.

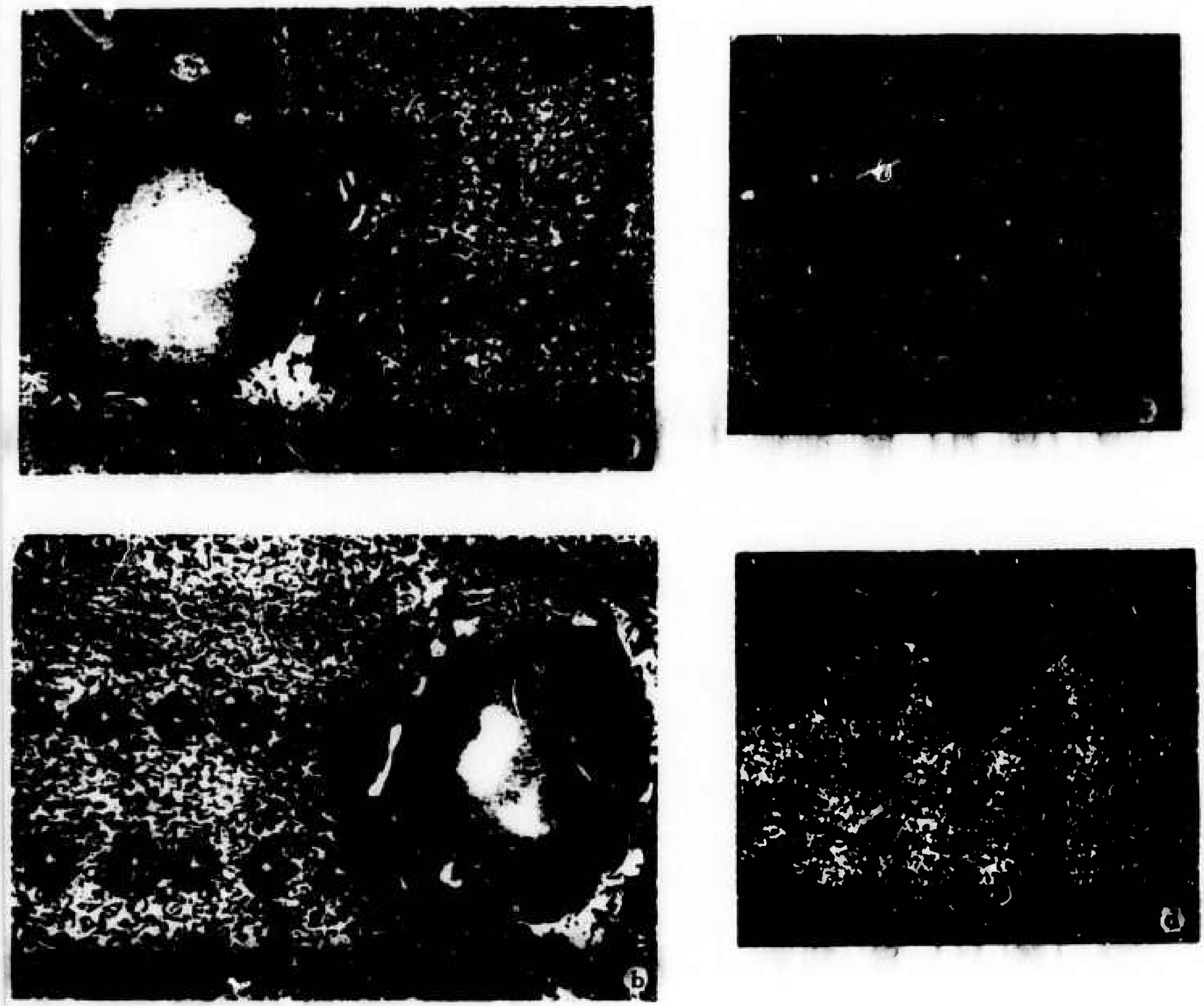

Fig. 1. Microstructure of alloy Al + 33.1% Cu in unstable (a, c) and stable (b, d) states.

a, b - Top view (x500); c, d - main cross-section (x300).

Table 1

Alloy	Crater depth, μm		Crater diameter, μm	
	Unstable	Stable	Unstable	Stable
Al + 11.7% Si	115	100	67	67
Al + 33.1 Cu	117	67	73	67
Al + 5.7% Ni	100	96	67	50

Microhardness of the specimens was measured in longitudinal sections and in radial directions from the crater. The value of microhardness was higher near the crater and decreased with the distance from crater walls. Microhardness of alloys in the unstable state was higher than in the stable state.

2) <u>Concentration Changes:</u>

Change of concentration was studied in these alloys: 66.9% Al + 33.1% Cu; 87% Ni + 13% Cu; 75% Ni + 25% Cu; 66% Ni + 34% Cu. Measurements were made with a MAR-1 micro-x-ray analyzer. Figs. 2 and 3 give concentration variations in stable and unstable states respectively, which show three characteristic portions in the stable and a single maximum in the unstable state.

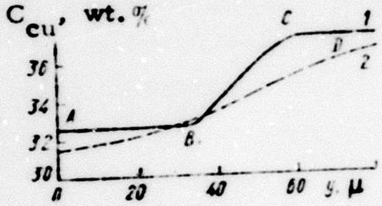

Fig. 2. Cu concentration variation in Al-Cu alloy, stable state.

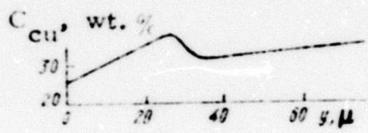

Fig. 3. Cu concentration variation in Al-Cu alloy, unstable state.

Karapetyan, R. V. and A. A. Samokhin. <u>Effect of bleaching on a regime of developed vaporization of metals by optical radiation.</u> Kvantovaya elektronika, no. 9, 1974, 2053-2055.

In laser evaporation of metals, at sufficiently high temperatures the conductivity of the liquid metal drops sharply and the depth of laser penetration in metallic targets increases. According to Batanov et al (ZhETF, 63, 1972, 586; IEEE J. Quantum Electronics, QE-9, 1973, 503), this drop in conductivity leads to the origin of "illumination waves" in liquid metals. Assuming this effect of illumination, the present authors show that in a steady-state regime, a totally illuminated layer of target, characterized by the

condition $y \ll 1$ (parameter $y = \alpha / \beta = \alpha \chi / v$, where α -absorption coefficient, χ - thermal conductivity, v- evaporation rate) is separated from the evaporation boundary by a thick optical layer, in which $y \gg 1$. Based on this finding, the authors observe that the origin of illumination effects cannot have any effect on the value of reflection coefficient R of incident radiation on a target, in the case of a stationary regime (stabilization time of the stationary regime may be 10^{-3} sec); this is in contradiction to the conclusion made in the work cited above by Batanov, et al.

The authors also point out that in the case of a semiconductor metallizing during fusion, it is possible to study the behavior of the fusion boundary according to the Doppler shift of radiation frequency in the far IR range, which passes through the solid semiconductor and reflects from the moving fusion front. Similarly, based on the character of the movement of a freely suspended target of a given mass, it would be possible to detect the increase in pressure during radiation interaction, which would indicate the limiting overheat temperature attained inside the liquid layer.

Kuz'michev, S. V., A. A. Uglov, and G. I. Fedotov. Kinetics of joint formation in thin plates welded by a pulsed laser. IAN B, no. 3, 1974, 60-63.

The present work investigates some problems in laser welding of thin metal plates, using a pulsed free-running laser. The test setup is shown in Fig. 1. Laser (LUCH-1M) radiation with $\lambda = 0.6943\ \mu$ and pulse duration $2\ \mu$sec was focused on the welding plate surface. Materials investigated were nickel plates being welded to a layer of titanium-copper alloy, deposited in vacuum by sintering on a ceramic base. Photographs of the processes were taken by a streak camera.

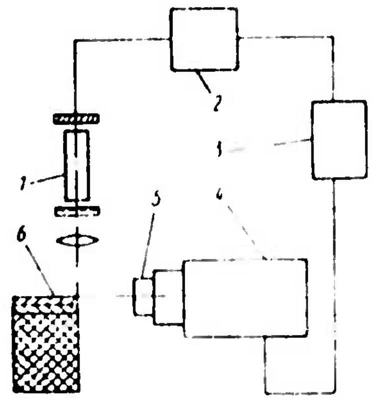

Fig. 1. Welding experiment

1- laser; 2- laser power pack; 3- SFR control panel; 4- SFR camera; 5- microscope; 6- Specimen (thin nickel plate, titanium-copper alloy layer; ceramic base).

Equations are developed for determining energy density I and radiation pulse energy Q for the case of pure fusion. Calculations conducted for a partial case (material-nickel; pulse duration $\tau = 2 \times 10^{-3}$ sec; focal spot diameter $d = 8 \times 10^{-3}$ cm) gave values of $I = 2.2 \times 10^{6}$ w/cm^{2} and Q = 0.22 joule, which are in good agreement with the experimental value of Q = 0.2-0.25 joule.

Qualitative evaluations are also given of the imperfection of contacts during laser welding. Experiments in this case were conducted with different combinations of plate thickness and external conditions (roughness, compression) at the welding specimen interfaces. The authors note that to obtain a high-grade weld of thin plates, it is necessary to obtain minimum possible thermal resistance of the contacts, by reducing the roughness of welding surfaces and the required compression.

A sufficiently strong joint at a given laser radiation pulse duration can be obtained by altering the energy density of the beam by slightly defocusing the latter over the welding plate surface, while maintaining its net energy at a calculated level.

Arifov, U. A., V. V. Kazanskiy, V. B. Lugovskoy, and V. A. Makarenko. D-c component of emission current, resulting from irradiation of tungsten by millisecond laser pulses. IAN Uzb, no. 4, 1974, 39-41.

A study is described on characteristics of emission current from a laser-irradiated metal surface. Specific attention was on the continuous current component, which is not a function of the integral heating of the irradiated specimen.

Emission was established with a ruby laser with spherical resonator. The laser was operated free-running with pulse duration at 2.5 μsec and energy of 1.7 joules. A tungsten target in the form of a disc of diameter = 10 mm and thickness of 1 mm was placed at a distance of 25 mm from the collector inside a glass vacuum vessel at a pressure of 2×10^{-6} torr. Radiation was focused by a lens with f = 70 mm.

Emission pulses from a 200 atm resistive load, placed in the target circuit and from an integrating RC-loop, placed in the collector circuit, were recorded by oscillograph. Collector potential with respect to the target was kept at +150 V. It was noted that in addition to intense spiked emission, a continuous component of the emission current was found to exist. (Fig. 1, Channels I and II). The time lag of the maximum continuous

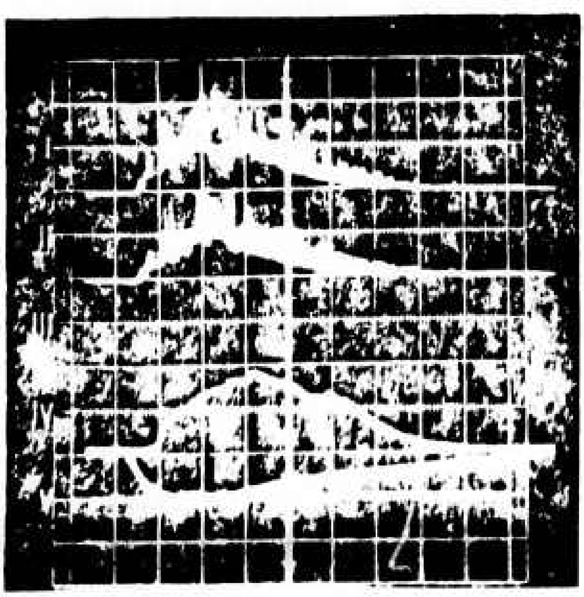

Fig. 1. Oscillogram of smoothed laser (V) and emission (IV) pulses, and emission current pulses in target circuit (I and II). Scanning velocity 260 μsec/cm.

current component relative to the laser radiation peak varied significantly from one exposure to another, but in all cases its value (0-260 μ sec) was less than the calculated lag value for the integral heating pulse; this in the absence of evaporation and for a constant reflection coefficient should theoretically be 750 μsec. Relationships were also obtained for amplitude values of the continuous current component as a function of radiation intensity (Fig. 2).

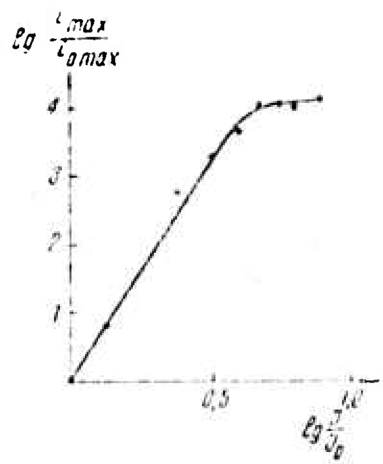

Fig. 2. Maximum constant component of the emission current i_{max} vs. radiation intensity I.

The authors suggest that the constant component of emission current could be the result of the superposition of spiked emission signals, and that its variation in time may be determined by the repetition frequency of the emission spikes. This constant emission current component is not a function of the integral heating of the target surface, and can be called a ghost or pseudointegral emission. The authors point out that the emission previously observed by French scientists Guathin et al. (Phys. St. Sol., 25 N2, 1968, 691), where a reference is made to the instability of time lags in emission current maxima, may be the same kind of emission as described in the present work.

Suminov, V. M., and V. I. Kachalin.
Technological feasibility for laser dimensional processing and the means of its realization.
EOM, no. 4, 1974, 33-38.

The article describes various methods of drilling holes by laser beam. They are identified as follows:

1.) Single-pulse drilling. Drilling is done by a single pulse from a solid-state laser, operating free-running with pulse energy = 10-100 joules. Accuracy of treatment for a specimen of roughness class 7 to 9 is class 3-4 radially and 4-5 axially.

2.) Multiple-pulse drilling. This method is applicable when it is necessary to obtain holes with a comparatively higher l/d ratio, or when using a laser with low energetic parameters (0.2-2 joules).

3.) Multibeam drilling. In this method, light radiation is divided with a beam splitter into a series of beams, which are then focused separately by lenses on the specimen surface, thus obtaining several holes at the same time. The source in this case is typically a solid-state laser with energy in the 10-100 joules range. Depending on the auxiliary power source, this method is subdivided into the following classes:

a). Gas-jet plus laser processing. In this case, in addition to the laser beam a supplementary gas jet is used, which helps in calibration of holes, removing ejecta from the laser treatment region, etc. This method produces holes of accuracy class 2 radially, improves the microgeometry of the surface to class 1-2, eliminates errors in lateral and longitudinal forms and solves technological problems in removing metal deposits from microhole channels.

b). Holes processing by light beam counter action. The supplementary source in this case is the feed-through optical flux which is reflected back to act again on the treated surface. This method permits changing the shape of the holes and also solves the problem of eliminating metal deposits in them.

c). Electric plus laser processing. This method uses the combined action of the laser beam and an electric discharge, which is initiated by the laser action. Its advantages are: removing more materials from the hole channel; removing projections from the treated specimen surface; eliminating closing of the hole; protecting the focusing lens from erosion products; obtaining hole diameters up to 2.5 mm; and metalizing simultaneously with hole drilling.

The authors further classify commercially produced Soviet processing lasers into three general categories and cite types of each. These are:

(1) Lab research types, e.g. the GOR-30 M;

(2) General purpose industrial use, e.g. the K3M, UL-20, Kvant-9 and -10;

(3) Special purpose industrial use, e.g. the ALA-1 (Fig. 1) and the semiautomated LP-2 (Fig. 2) for precision hole drilling to 0.5 mm diameter.

Fig. 1. ALA-1 Laser drill.

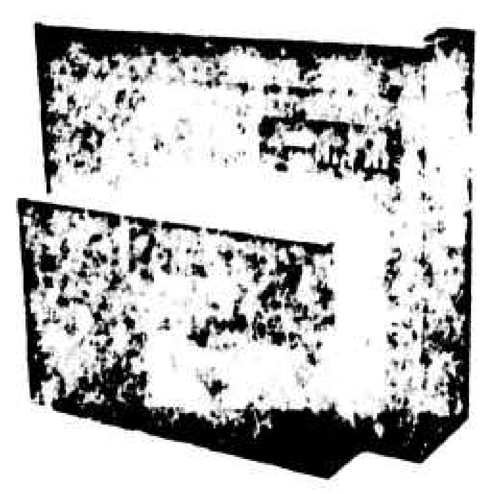

Fig. 2. LP-2 Laser drill.

Bystrova, T. V., G. I. Kozlov, V. A. Kuznetsov, V. I. Lisitsin, and V. M. Trishkin. Combined laser-gas cutting of metals. FGiV, no. 6, 1974, 857-864.

Laser-gas cutting of metals consists of the combined action of a focused laser beam and gas jet on a metal surface, leading to fusion (destruction) of the material and hydrodynamic separation of it from the cutting zone. In this method, all laser radiation power is concentrated on a very small surface area of the material, e.g. dimensions = 0.1-0.3 mm, thereby obtaining a high flux density of the order of 10^6 w/cm^2, which allows for very narrow cuttings with high quality edges and small regions of thermal effects. Three methods of laser cutting are outlined:

1. At high laser radiation power, cutting can be done by laser beam energy alone.
2. At medium powers, laser plus gas cutting is applied, where the energetic process is determined by laser radiation and a chemical source.
3. Cutting is possible also by the exothermic reaction of metal burning under the action of a gas jet, reacting with the metal; laser radiation only initiates the process.

Experiments were conducted with stainless steel (1Kh18N9T), chrome-nickel-titanium steel with copper (VNC-2), nickel based alloy (EI-602) and chrome-nickel-molybdenum steel (SN-3). Figure 1 shows the experimental sketch. A high-powered (CO_2+N_2+He) laser was used with a beam diameter of 50 mm,power = 980 w and divergence = 10^{-3} rad. Maximum cutting rates were determined as functions of specimen thickness, laser radiation power and oxygen consumption. Cutting rates for different materials as a function laser radiation power are shown in Fig. 2.

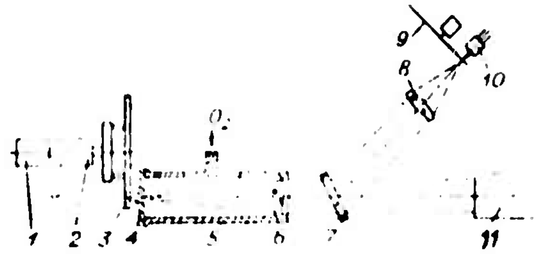

Fig. 1. Cutting experiment.

1- Electric motor; 2- reducer; 3- specimen; 4- nozzle; 5- input attachment; 6- laser beam lens; 7- splitter; 8- lens; 9- shutter; 10- counter; 11- laser.

Fig. 2. Cutting rate as a function of laser radiation power.

1- 1Kh18N9T, thickness 2 mm; 2- SN-3, thickness 1.5 mm; 3- VNS-2, thickness 1.5 mm; 4- EI-602, thickness 1.0 mm.

It is seen that for materials under similar thermophysical conditions, cutting rates at different conditions remain very close. Cutting rate is seen as strongly dependent on specimen thickness. At laser power 800 w and oxygen consumption ~ 30 liter/min, the rate for laser-gas cutting of stainless steel of thickness 1 mm was ~ 5 m/min. Relationships were determined for the cut width as a function cutting rate. Experiments were also conducted to study effects of laser-oxygen cutting on the microstructure of titanium, in the thermally affected regions.

Based on a thermohydrodynamic model of laser-gas cutting, an expression is developed for determining cutting rate. Calculated results are found in good agreement with experiments. Calculations shows that the incident flux is related to specimen thickness by $q \sim d^{-1}$; while for density of heat flux due to chemical reaction in metal oxidation, $q_x \sim d^{-3/4}$.

Uglov, A. A., and V. A. Kondrat'yev. Laser welding of thin conductors made of refractory materials. FiKhOM, no. 6, 1974, 7-11.

Adjoining thin conductors of BP5 and BR20 alloys (diameters 100 and 350 μ) were exposed to pulsed ruby laser radiation with a power density of 2×10^5 w/cm^2. The conductors were oriented in different positions with respect to the laser beam direction (Fig. 1). The dependence of the volume

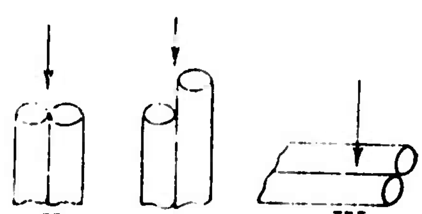

Fig. 1. Orientation of conductors with respect to laser beam.

of the melt zone on exposure time is shown in Fig. 2.

The experiments show that the formation of a welded joint, which is completed before termination of the laser pulse action, is accompanied by ejection of a liquid phase fraction, but no evaporation or gravity effects.

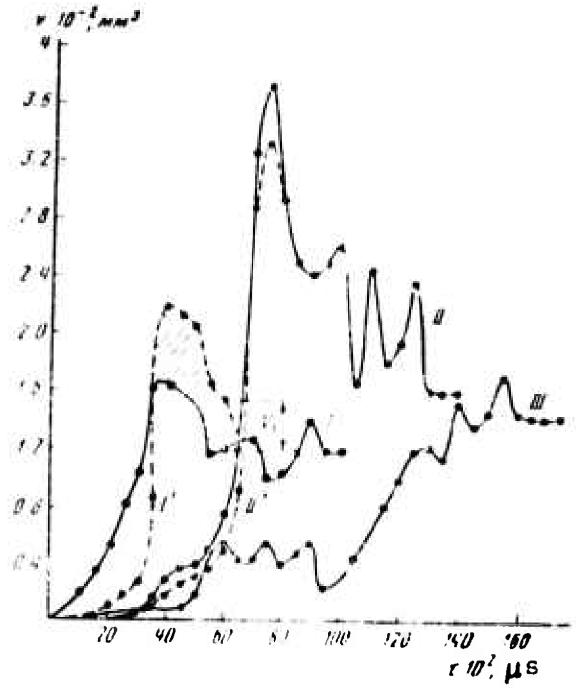

Fig. 2. Dependence of the volume of melt zone on exposure time for the cases shown in Fig. 1.

In the case I (Fig. 1) (differential length ~ 200 μ), melting of the end planes begins simultaneously. After a certain time, the two melt zones fuse and a common welding bead forms, which is accompanied by ejection of a liquid phase fraction. The observed phenomenon was explained by the release of surface energy during fusing of the two melt zones.

2. Dielectric Targets

Aleshin, I. V., L. V. Aleksandrova, A. M. Bonch-Bruyevich, Ya. A. Imas, and A. K. Yakhkind. Effect of chemical processing on the optical breakdown threshold of a glass surface. ZhTF, no. 1, 1975, 200-203.

Results are described of experimental studies on effects of different methods of treating glass surfaces on their laser breakdown threshold. Glass specimens used were types K-8 and TK-16, and the methods of their surface treatment were: (1) Normal mechanical grinding and polishing (NGP); (2) High grinding and polishing (HGP); (3) HGP + ion polishing (IP); (4) NGP + etching in nitric acid solutions; (5) NGP + etching + chemical treatment with sulfur hexafluoride.

Threshold tests were conducted at two laser wavelengths, $\lambda_1 = 0.69$ and $\lambda_2 = 1.06\ \mu$ in regimes as shown in Table 1.

Table 1. Laser operation regimes

Number of Regime	Operation regime	Laser wavelength, μ	Pulse duration, sec	Focal spot diameter, cm
1	Single-pulse	0.69	$2 \cdot 10^{-8}$	$3 \cdot 10^{-2}$
2	Single-pulse	1.06	$2 \cdot 10^{-7}$	$3 \cdot 10^{-2}$
3	Quasicontinuous	1.06	10^{-3}	$3 \cdot 10^{-2}$
4	Quasicontinuous	1.06	10^{-3}	0.6

Regime # 1: - Commercial ruby laser, type GOM-1 with f = 10 cm

Regime # 2 and 3: - Nd laser with unstable resonator and electrooptical modulator, f = 40 cm.

Regime # 4: - Nd laser in quasicontinuous free-running regime with spiked modulation < 20%.

Table 2

Threshold surface breakdown for different methods of surface treatment

No.	Methods of treatment	Surface breakdown threshold, joule/cm^2	Threshold breakdown in relation to that of NGP treatment
1	NGP	34 ± 2	1.0
2	NGP	52 ± 3	1.53
3	NGP + IP	67 ± 3	1.97
4	NGP + etching	42 ± 2	1.31
5	NGP + etching + SF_6	69 ± 3	2

Table 3

Effect of chemical treatment on threshold breakdown at different laser regimes

Glass Specimen	Laser operation regime	Relation between threshold breakdowns for chemical treatment and HGP
TK-16	# 2	1.2
K-8	# 2	1.2
K-8	# 3	1.0
K-8	# 4	0.8

Table 2 shows the results of different methods of surface treatment, while Table 3 shows effects of chemical treatment on the threshold breakdown in different regimes of laser operation. It is seen from the tables that threshold optical breakdown of glass surfaces subjected to treatment with SF_6 increases only in the range of laser pulse durations $< 2 \times 10^{-7}$ sec. This effect is seen to disappear with the increase of pulse duration. A brief discussion is given of the above experimental results, based on the presence of absorbing inhomogeneities in the target glass.

Kikin, P. Yu., and V. I. Paramonov. Effect of a facet of a ruby crystal on its internal breakdown. Kvantovaya elektronika, no. 9, 1974, 2092-2094.

Interaction of laser radiation with facetted ruby crystals was experimentally studied. Ruby rods of 6.5 mm diameter and length = 80 mm were used, with Cr^{3+} concentrations of 0.018 to 0.025%. The optical axis was at 60 to 65° to the rod axis. Side surfaces were polished thermally in vacuum at 1900 to 1980° C. The output faces of the leucosapphire tips were polished by diamond powder, to a smoothness of ∇13. Facets of the ruby crystal were 0.1 - 0.2 mm wide and their surface smoothness was ∇10 - 12; they were inclined at angles 45 - 50° to the generating line (Fig. 1). A Q-switched He-Ne laser was used for irradiation, with energy output = 0.2-0.3 joule and pulse duration = 20-30 nsec.

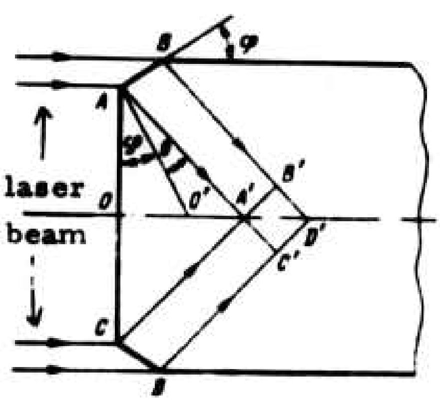

Fig. 1. Laser beams passing through crystal facets.

AB, CD- facets; AC- end face; A'B'C'D'- destruction region.

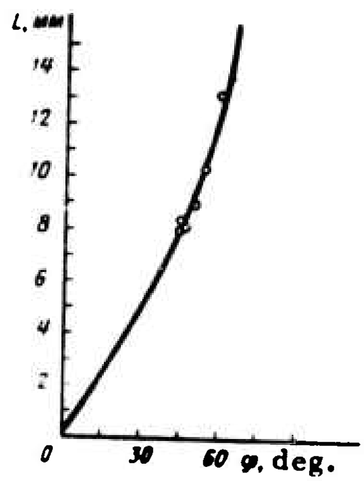

Fig. 2. Damage depth vs. angle.

Damage in the form of spherical cavities was seen to occur inside the ruby crystal due to the interaction of laser radiation with inhomogeneities present. Damage area diameter equalled 0.4 mm and was consistently located near

the crystal axis at 8-10 mm from the end face. Damage location inside the crystal depended on the facet angle φ (Fig. 2), although its character remained constant. Damage did not occur in crystals with dull facet surfaces up to $\nabla 8$.

Uglov, A. A., and D. I. Cherednichenko. Thermal stresses in transparent plates from the effect of laser radiation. FiKhOM, no. 4, 1974, 126-128.

Thermal stresses generated by laser irradiation of transparent plates were investigated previously by Andreyev and Ulyakov (I-FZh, v. 15, no. 6, 1968, 1093), where destruction threshold values were determined of radiation density for a number of materials. It was shown that stress levels over a wide range of specific power were sufficiently great to cause intensive destruction in the interaction region.

In the present work, the authors show that estimation of such stresses can be significantly simplified and determined without using any mathematical simplifications, if the Gaussian distribution of specific power over the laser beam cross-section is taken into account. Plates of finite thickness are considered, and solutions to quasistatic problems of thermoelasticity during local laser interaction are obtained with the use of Green's function and the Gaussian law. Based on the obtained relations, quantitative analyses are conducted for the thermal stresses in irradiated plates. Graphical solution shows that all stresses are localized around a maximum at the center of the beam interaction zone, and sharply decrease with distance from the crater impact point. All stresses in the thermally active zone are compression, but at points sufficiently remote from the radius of beam interaction, stress reverses sign and becomes tension.

Danileyko, Yu. K., A. A. Manenkov, V. S. Nechitaylo, and A. I. Ritus. Role of absorbing defects in the mechanism of laser destruction of real transparent dielectrics. Kvantovaya elektronika, no. 8, 1974, 1812-1818.

The laser destruction mechanism of various transparent dielectrics was investigated with special attention to the criteria of optical purity, self-focusing effect, and the role of microdefects in destruction. Experiments were done with a single-frequency ruby laser having a variable pulse duration in the 1-7 nsec range. A He-Ne laser was used as a probe for indicating the possible presence in specimens of large defects and impurities, as well as the onset of destruction. The experimental setup is shown in Fig. 1. Specimens used were sapphire and quartz crystals, and glasses including type TF-8 heavy flint, BK-104 barytic crown, K-8 optical glass and laser glasses (not specified).

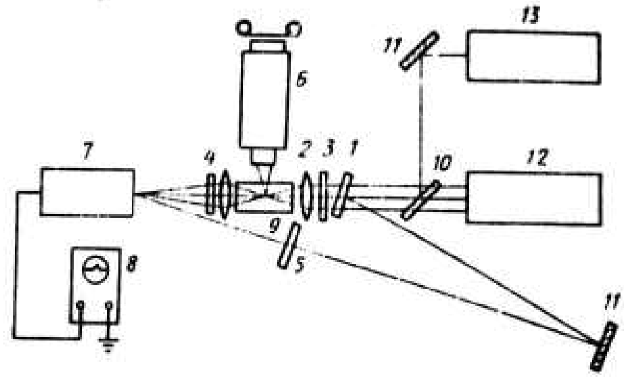

Fig. 1. Dielectric breakdown experiment.

1 - Splitter for optical delay of incident radiation pulse; 2- focusing lens; 3, 4, 5- neutral filters; 6- microscope for observing spatial structure of luminescence and light scattering from the caustic of focusing lens; 7- photo deflector; 8- high-speed oscillograph; 9- specimen; 10- splitter; 11- mirror; 12- ruby laser; 13- He-Ne laser.

Based on a comparison of intensities of the Rayleigh and Brillouin scattering, criteria for the optical purity of transparent dielectrics were examined. Tabulated experimental results list damage thresholds ranging from 130 kw for sapphire down to 10 kw for type TF-8 glass. The results confirm that even the purer forms of optical specimens contain a significant quantity of absorbing defects, which play an important role in the process of laser destruction. Destruction in such materials occurs through a stage of self-focusing, which seems to be the limiting factor for determining their optical stability.

The authors emphasize that the problem of the actual mechanism in laser destruction, which determines the limiting stability of transparent dielectrics, remains open. In any theoretical analysis of this mechanism, it is necessary to take absorbing defects into account, which are always present in real media.

Zakharov, S. I., Yu. N. Lokhov, and Yu. D. Fiveyskiy. Generation of shock waves in an optically transparent dielectric by a focused laser pulse. FiKhOM, no. 4, 1974, 16-21.

Generation of shock waves in an optically transparent dielectric by a focused laser pulse is discussed, based on an efficient explosion model. The amplitude and velocity of shock waves formed at the focal region boundary and their relationships with energy absorbed in the focal region are evaluated. Laws of shock wave attenuation are obtained for various geometries of laser radiation. The possibility of shock wave generation with an acoustic precursor is considered for the case of solid dielectrics; critical energy flux density absorbed in the focal volume is determined in relation to the formation of a two-wave regime and "ordinary" shock waves.

Calculated and theoretical thresholds for selected materials are shown in Tables 1 and 2. Theoretical threshold for K-8 glass, $E_a \sim 0.04$ joule,

Table 1

Thresholds of plastic shock wave formaton in solid dielectrics, and luminescence threshold at shock wave front in sapphire

Material	Hugoniot elastic limit p_a, kbar	Shock wave formation threshold $E_a \times 10^3$, joules	Shock wave formation threshold $W_a \times 10^{-10}$ w/cm^2
PMMA	7-8	1	0.1
TF-5 Glass	80	9	0.9
K-8 Glass	90	12	1.2
Sapphire	120 (200)	16 (27)	1.6 (2.7)
	Luminescence of sapphire	Luminescence threshold, E_n	Luminescence threshold, W_n
	p = 150 kbar	20×10^{-3} joule	2×10^{10} w/cm^2

Table 2

Threshold of shock wave formation with velocity $D > C_1$.

Material	Boundary of two-wave region. (Shock wave amplitude) p_s, kbar	Threshold in absorbed energy E_a, joule	Threshold in absorbed power. $W_a \times 10^{-10}$, w/cm^2
TF-5 Glass	170	0.02	2
K-8 Glass	250	0.04	4

agrees well with previous experiments, where the shock wave formation threshold for $D > C_1$ (D-Shock wave velocity, C_1- velocity of linear elastic waves) was $\sim$ 0.05 joule. Shock waves attenuate comparatively quickly, such that at an amplitude $\Delta p \sim 6 \times 10^5$ atm in cylindrical geometry, plastic shock waves attenuate at a distance $r \sim 14\ r_o$ (r- radial coordinate in focal

volume; r_0 : d/2, d- characteristic dimension of focal region). The formation of shock waves takes place until the development of breakdown. Generation of shock waves (with sufficient amplitude) can cause material destruction in the focal region, as diverging compression waves carry away matter with them, and a critical stress can occur.

Attention should be given to experimental determination of the focal volume V_f, since a strong increase of V_f with increase in E_a due to the mechanism of "moving focus" can, in principle, restrict the level of pressure generated in a dielectric volume by a laser.

The authors also note that since the two-wave configuration occurs near any phase transition point, the cited method of shock wave formation by laser can be used for investigating phase transitions of a substance.

Zhdanovskiy, V. A., and V. N. Snopko. Investigation of a plasma, formed by laser action on a dielectric. FiKhOM, no. 4, 1974, 12-15.

Parameters were investigated of plasma, generated from vapors of various dielectrics under laser irradiation. Experiments were conducted according to the sketch of Fig. 1. A CO_2-N_2-He laser (proportions 1:2:7) was used for specimen irradiation, operating in a multimode regime with

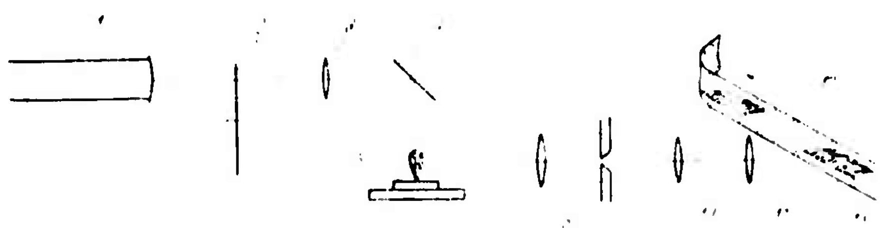

Fig. 1. Experimental sketch.

1- laser; 2- modulator; 3- lens; 4- mirror; 5- specimen; 6- stand; 7- flare; 8- lens; 9- hole (dia-0.20 mm); 10- lens; 11- objective; 12- high-speed film; 13- time photoscanning.

controlled power up to 100 w. Target specimens used were glass, quartz, textolite, laminated bakelite insulation, ebonite, and others. Processes of plasma generation were recorded on high-speed photographic film.

Photographic scanning showed that evaporation of target materials under laser radiation had a pulsating character. Specimens were heated to a depth not more than 0.2 mm and the laser focal spot diameter on the specimen surface was 0.3 and 0.6 mm. Pulsation frequency was of the order 10^3-10^4 Hz. Thermal destruction products of specimens generated flares, oriented normal to the specimen surface. The velocity of vapor expansion inside the flare was found to be subsonic, and was about two times greater than the velocity of the flare front. Velocity of the flare front was a function of the incident radiation power. Flare temperature was found to be about 4000° K.

The article includes a plot of flare expansion velocity as a function of its height above the specimen surface. Qualitative spectral analyses were also made of the flares.

Khazov, L. D., I. A. Fersman, and V. Yu. Bortniker. Cumulative effect of the destruction of transparent dielectrics from multiple irradiation by a laser. ZhTF, no. 9, 1974, 2020-2022.

Laser destruction of K-8 glass with a standard polished surface was experimentally studied. Along with longevity, scattering of laser light on the specimen surface was investigated in order to explain the causes for weakening of surface optical strength after multiple irradiation. A sketch of the experiment is shown in Fig. 1, and experimental procedures are outlined.

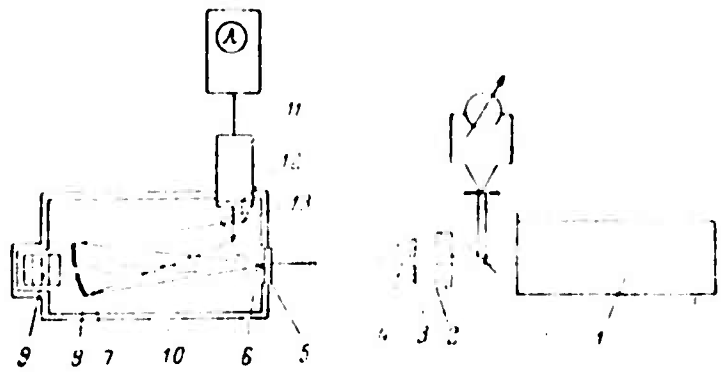

Fig. 1. Destruction experiment.

1- Single-pulsed single-mode ruby laser; 2- neutral light filter; 3- diaphragm; 4- collecting lens; 5- specimen; 6- blackened cone; 7- tube; 8- concave mirror; 9- cassette with neutral light filter; 10- housing; 11- photomultiplier; 12- NS-9 and KS-19 filters; 13- prism.

Relationships are found for the number of laser flashes N to destruction as a function of beam energy density W (Fig. 2). At a beam energy

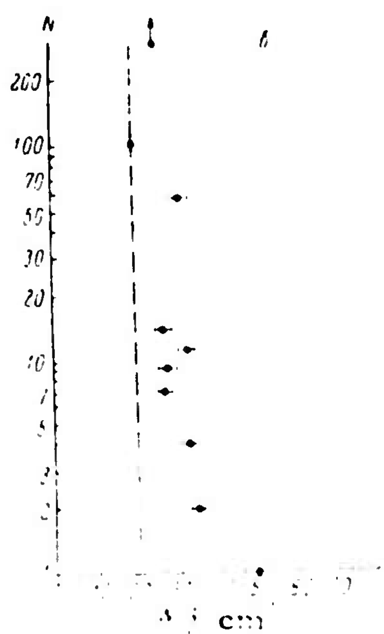

Fig. 2. Number of laser flashes N to destruction, as a function of beam energy density W.

density $W = 29$ joules/cm^2 (irradiations were conducted at seven different levels), destruction of the specimen did not occur even after 100 shots. Optical scattering signals, as recorded in an oscillograph, were found to increase gradually with the increase of N prior to destruction. This growth in signal scatter indicates the cumulative formation of microdefects on the specimen surface layer as a result of multiple shots, causing aging of the specimen and weakening of its optical stability.

The authors conclude that it is possible to obtain a value of beam energy below which destruction does not take place even for arbitrarily large N. This is called the reliability limit of a given specimen (e.g. the dotted line in Fig. 2). It would be necessary to conduct thousands of laser shots for determining this limit, which was impractical in the present test program.

Leonov, R. K., V. V. Yefimov, S. I. Zakharov, N. F. Taurin, and P. A. Yampol'skiy. Study of effects resulting from focusing of a Nd laser single pulse at a glass-liquid interface. ZhTF, no. 1, 1975, 130-133.

Leonov, R. K., N. F. Taurin, K. B. Sherstnev, and P. A. Yampol'skiy. Role of cavitation in the optical breakdown of a glass surface contacting a liquid. FiKhOM, no. 6, 1974, 134-136.

The authors investigate certain peculiarities of optical breakdown at a glass-liquid interface during focusing of a Nd laser pulse. The Nd laser single pulses of $\tau = 40$ nsec duration were focused on the surface of a glass specimen which was placed in contact with distilled water, as shown in Fig. 1a. Energetic and power thresholds were measured of the optical surface destruction.

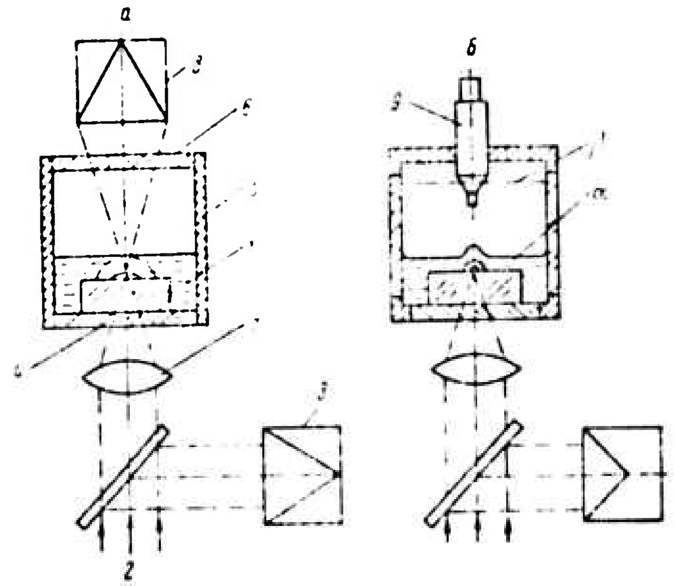

Fig. 1. Experimental sketch.

a) Measurement of the surface destruction threshold of glass specimens; b) Split-off scheme of measuring mass velocity using a sensor.

1- specimen; 2- laser pulse; 3, 8- calorimeters; 4- input window; 5- vessel; 6- plane window; 7- lens; 9- waveguide sensor.

The destruction threshold was found to depend on dimensions of the focal spot, increasing with decrease of focal spot diameter. In the case of a K-8 glass specimen, the surface destruction threshold decreases from Q = 65 to Q = 25 joules/cm^2 with increase of focal diameter d_f from 0.32 to 1.15 mm, which corresponds to an increase of focal spot area by more than 10 times. Energy loss in the focal volume during breakdown likewise increased with increase of d_f. At d_f = 0.55 mm, energy loss in the focal volume equals about 0.2 joules. Insertion of the glass specimen in water increases the surface breakdown threshold of the former, relative to its threshold in air.

Experiments were similarly conducted for determining parameters of shock waves generated in the water at threshold conditions by means of contact (using waveguide sensors) and 'split-off' (using waveguide sensors and high-speed shadow photography) methods (Fig. 1b). Based on the approximation of adiabatic shock compression, the parameters of these shock waves are theoretically estimated and their attenuation processes near the focal volume are discussed. Calculated amplitudes of pressures are found in good agreement with experimental results, obtained at a sufficient distance from the focal volume by both above methods. At small distances the contact method is found not applicable.

Data from the same type of test is also presented by the authors in the second cited paper.

Yepifanov, A. S. <u>Avalanche ionization in solid transparent dielectrics induced by strong laser radiation pulses.</u> ZhETF, v. 67, no. 5, 1974, 1805-1817.

A theoretical mechanism for laser breakdown of dielectrics is proposed. The breakdown sequence is treated as follows. As a result of multiphonon ionization of valence electrons, added electrons appear in the conduction band. During the laser pulse these are accelerated to above-ionization energies and start an avalanching process. If during the pulse the density of excited electrons passes some critical level at which absorbed energy induces irreversible processes, then damage is considered to have occurred.

The author develops a general method for solving kinetic equations which define the onset of the avalanching process, the critical value of exciting optical field, and the temperature relationship of these parameters. The treatment also defines the energy transmitted to the lattice by excited electrons, thus enabling the formulation of a physically supportable criterion for optical destruction.

Formulas are derived defining the relationship between the constant of avalanche ionization, γ , and the electric field E in light waves at $\hbar \omega << I$, where I is ionization potential. An analysis is also given of the temperature dependence of the critical electric field, energy absorption by the electrons in the conduction band, heating of the crystal lattice, and spatial diffusion of electrons. A meaningful criterion for optical breakdown, $\gamma \tau$, is thus formulated. Numerical estimates are given for the critical electric field in the visible region of the spectrum and for the duration of avalanche ionization.

Kovalev, V. I., V. V. Morozov, and F. S. Fayzullov. Occurrence of opacity and breakdown of optical materials under pulsed CO_2 laser radiation. Kvantovaya elektronika, no. 10, 1974, 2172-2177.

The threshold intensity of opacity onset for various materials used in infrared optics were measured under laser exposure. CO_2 laser radiation was characterized by a pulse energy of 350 mj and power of 0.5 Mw (Fig. 1). The method of measurement used enabled the authors to determine

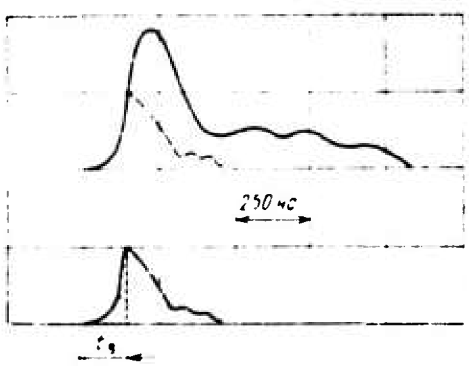

Fig. 1. Oscillograms of laser pulse before (above) and after (below) passing through a sample.

the threshold intensity corresponding to the moment of opacity onset in each pulse.

The threshold intensities for surface and internal opacity are given in Table 1. The appearance of the internal opacity was accompanied

Table 1

No.	Material	Threshold intensity, Mw/cm^2	
		Internal	Surface
1	NaCl	170	65
2	NaCl	290	60
3	NaCl	500	90
4	KRS-5	90	60
5	KRS-6	110	40
6	BaF_2	1000	47
7	BaF_2 (plate)	-	55
8	Ge (plate)	-	50
9	ZnSe (plate)	-	57

by breakdown in the form of cracks in cleavage planes in the case of NaCl and BaF_2, or in the form of puncture marks with KRS-5 and KRS-6 (not identified). The appearance of surface opacity was accompanied by breakdown only in the case of BaF_2, Ge and ZnSe. The surface of NaCl, KRS-5 and KRS-6 become more transparent under the effect of laser irradiation, and after repeated irradiation, the opacity threshold increased as shown in Table 2.

It was concluded thatthe surface opacity threshold for some infrared materials is determined by breakdown of air in vapor

Table 2

Threshold intensity after repeated exposure, Mw/cm^2

No.	Material	Number of shots					
		1	2	3	4	5	6
2	NaCl	60	90	115	120	145*	-
2	NaCl	55	83	120	130	136	160*
3	NaCl	90	240	300	360	410*	-
5	KRS-6	40	60	90*	-	-	-
5	KRS-6	40	80	83	96*	-	

* Asterisk indicates onset of surface breakdown

contaminating the surface. Certain materials (NaCl, KRS-5 and KRS-6) thus can be decontaminated by laser irradiation.

Gridin, V. A., A. N. Petrovskiy, and S. L. Pestmal. Features in the breakdown of transparent solid media by an ultrashort laser pulse. Kvantovaya elektronika, no. 10, 1974, 2278-2281.

The dynamics of laser-induced filamentary cracks in KDP crystals were studied and breakdown thresholds were compared at $\lambda = 1.06\ \mu$ and $0.53\ \mu$ for fused quartz, K-8 glass and KDP crystals. Tests were done with a mode-locked Nd glass laser with a repetion period of 8 nsec, pulse energy of 0.04 j, and pulse duration of 4-8 psec, using the method of shadow photography (Fig. 1).

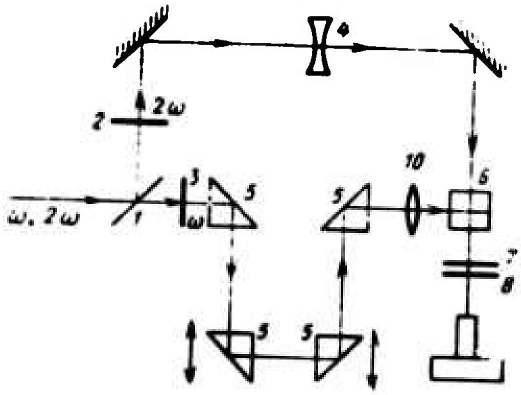

Fig. 1. Experimental setup.

Typical cracks in KDP crystals are illustrated in Fig. 2.

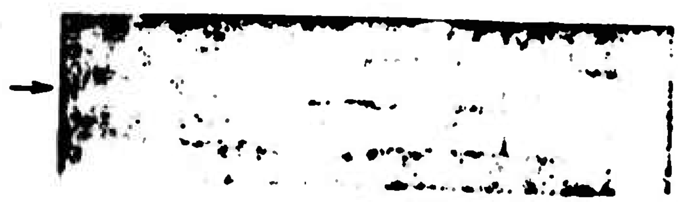

Fig. 2. Typical filamentary damage in KDP, X20. Arrow shows beam direction.

They propagate both in and opposite to the direction of laser propagation, the former ceasing the more rapidly. The breakdown threshold was found to be lower at $\lambda = 0.53\mu$, i.e. by a factor of two for K-8 glass and fused quartz, and a factor of four for nonlinear KDP crystals (in agreement with results of Belozerov et al., 1972, but in contradiction to Zveryev et al., 1973 and Bayev et al., 1974). This phenomenon is suggested to be associated with multiquantum processes in the absorption of radiation energy.

The authors note that their experimental techniques did not provide a control of the pulse duration, nor a study of the dynamics of self-focusing. These factors thus precluded any comparison between the present results and a self-focusing model of crack propagation.

Kanayev, I. F., and V. K. Malinovskiy.
Mechanism of optical damage of electrooptic crystals. FTT, no. 12, 1974, 3694-3696.

The dynamics of laser-induced change in refraction index were studied by a holographic method. Tests (Fig. 1) were conducted using

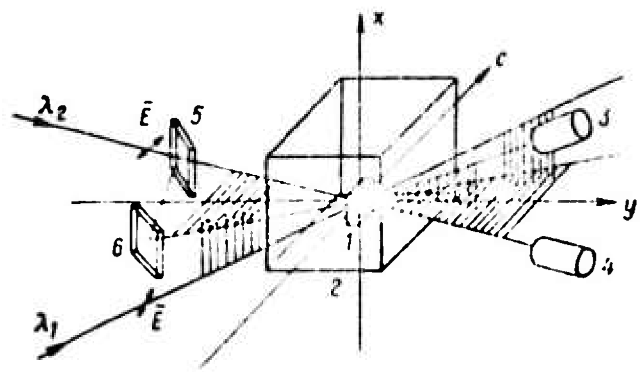

Fig. 1. Experimental setup.

1- $LiNbO_3$ crystal (c - optical axis); 2- thermostat (-60 to + 60° C); 3, 4- photomultipliers; 5, 6- beam splitters.

$LiNbO_3$ crystals set in a thermostat which were exposed to a single-pulsed Q-switched ruby laser ($\tau = 30 \times 10^{-9}$ sec). A He-Cd laser beam probe ($\lambda_1 = 0.44\ \mu$, power = 10 mw) was diffracted and Δn was determined from diffraction efficiency. Test results are exemplified by Fig. 2.

Results show that the refraction index changes only during the action of the laser pulse, and its time variation does not depend upon the temperature of the target. The time variation of the diffraction efficiency is adequately represented by the function $E = \int_0^t I(t)dt$, where I(t) is the intensity of incident light (Fig. 2, c).

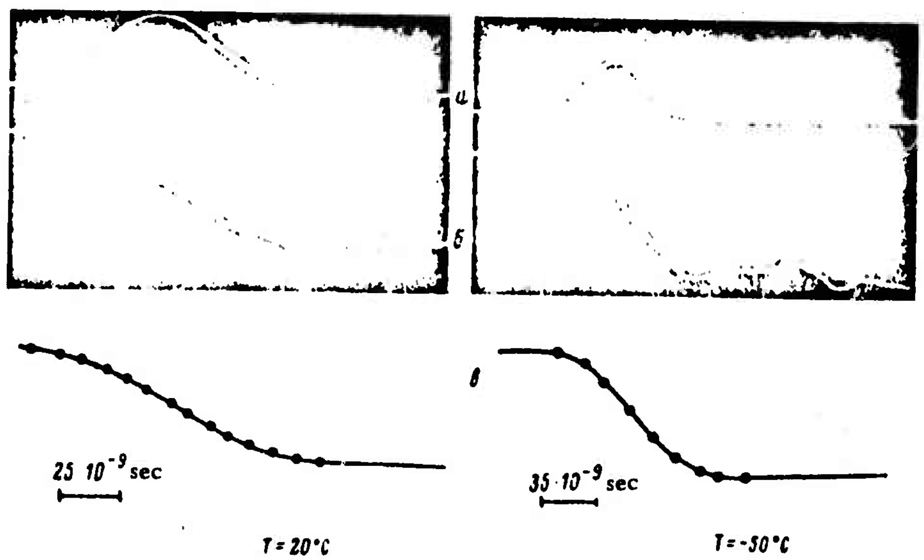

Fig. 2. Ruby laser pulses (a) and diffraction efficiency (b) at temperatures of 20° C and -50° C.

The authors suggest that optical damage of electrooptic crystals is associated with a laser-induced change of spontaneous polarization, and not with an electrooptical effect as suggested by some authors.

Bonch-Bruyevich, A. M., Ya. A. Imas, A. A. Kovalev, P. S. Kondratenko, and B. I. Makshantsev. Laser-induced surface evaporation of a solid transparent dielectric. ZhTF, no. 11, 1974, 2393-2397.

The problem of laser-induced surface evaporation of a solid transparent dielectric was solved theoretically under two separate limiting conditions, namely a quasiclassic electromagnetic field and a strong reflection of light from the front of the absorption wave. The surface temperature and the evaporation rate were also numerically estimated for the latter case.

The temperature T(r, t) is defined by the following system of equations:

$$\frac{\partial T}{\partial t} = \chi \Delta T + g(T, |\mathbf{E}|^2), \tag{1}$$

$$\Delta \mathbf{E} + \left(\frac{\omega}{c}\right)^2 \epsilon(T)\mathbf{E} = 0. \tag{2}$$

Here χ is thermal conductivity; $g(T, |\mathbf{E}|^2) = (\omega/8\pi c)\,\mathrm{Im}\,\epsilon(T)\,|\mathbf{E}|^2$; where ω is laser radiation frequency, c is velocity of light, and $\epsilon(T)$ is complex dielectric permeability given in the form

$$\epsilon(T) = 1 - \frac{\tilde{\omega}^2 e^{-I/T}}{\omega^2 + \nu^2}\left(1 - \frac{i\nu}{\omega}\right), \tag{3}$$

where $\tilde{\omega}\, e^{-I/T}$ is plasma electron frequency and ν is electron collision rate. Since the solution of Eqs. (1) and (2) is sought in the region near the intersection of the light propagation direction and the dielectric surface, and for times where the width of the temperature front near the surface is smaller than the curvature of the temperature front, the problem can be considered as one-dimensional. The solution obtained was found to be stable.

For the case of strong reflection of light from the front of the absorption wave, the following expressions were obtained for the surface temperature and evaporation rate

$$T_1 = \frac{I}{\ln\sqrt{\frac{q_0}{q}} + \ln\ln\sqrt{\frac{q_0}{q}}}, \tag{4}$$

$$v = \frac{2s\sqrt{\frac{q}{q_0}}}{\ln\frac{q_0}{q}}, \tag{5}$$

where

$$q_0 = \frac{I s^2 c \tilde{c}}{\text{[illegible]}}. \tag{6}$$

For $I \gtrsim 4 \times 10^4$, $S \gtrsim 10^5$ cm/sec, $\tilde{c} \gtrsim 1$ j/cm^3/$^\circ$C, $\varkappa \gtrsim 10^{-2}$ cm^2/sec, $\nu \gtrsim 10^{14}$ sec^{-1}, $\lambda \gtrsim 3 \times 10^4$ and $q \gtrsim 10^8$ w/cm^2 the surface temperature and evaporation rate are found to be $T_1 \approx 8 \times 10^3$ $^\circ$C and $v \approx 10^2$ cm/sec. This result agrees with experimental data of Aleshin et al. (ZhTF, 1971, 820).

Kovalev, A. A., and B. I. Makshantsev. Role of nonradiative transitions during propagation of optical absorption waves in a solid transparent dielectric. FTT, no. 1, 1975, 188-193.

An analysis is presented on the problem of propagation of high-temperature optical absorption waves in a solid transparent dielectric exposed to laser radiation. Studies are made for the case in which two levels with excitation concentrations n_1 and n_2 in the upper and lower state respectively exist near the bottom of conductivity zone, and intensive transitions take place between these two levels owing to laser irradiation. These nonradiative transitions between excited states are assumed to be the main source of heat.

The possibility of the absorption and stimulated emission of light per unit time during these transitions is $\sigma q(r)/\hbar\omega$, where σ = absorption cross-section of a light quantum with frequency ω, and $q(r)$ = radiant power density at a point with radius vector r. The problem is solved theoretically, assuming strong laser reflection from the absorption wave front, resulting from a sufficiently high concentration of free electrons. Expressions are derived for maximum temperature and propagation velocity of the absorption waves as functions of radiant power density. Calculations show that the maximum temperature in the absorption wave is of the order of 10^4 $^\circ$K and its velocity $v = 10^3$ cm/sec.

Kaczmarek, F., and E. Pawlowska. Electric breakdown in KDP crystals at optical frequencies. Optica applic., v. 3, no. 2, 1973, 57-58. (RZhRadiot, 8/74, #8Ye263). (Translation)

Threshold flux density of powerful laser radiation causing electric breakdown in KDP crystals was measured. A Q-switched ruby laser was used as the radiation source. Crystal damage at breakdown was considerable. Threshold breakdown energy was of the order 0.33 joules, which corresponds to a power density of 105 Gw/cm^2. Experimental values could not be compared with theoretical data owing to the absence of the latter.

3. Semiconductor Targets

Manenkov, A. A., G. N. Mikhaylova, A. S. Seferov, and V. D. Chernetskiy. Studying superheating effects in germanium specimens under the action of laser radiation in liquid helium. FTT, v. 16, no. 9, 1974, 2719-2724.

Effects of overheating were studied in Ge specimens in conditions of both pulsed and c-w laser excitation at T = 1.3°K in He^3 and He^4. Experiments were done with a superconducting Al bolometer fixed to the specimen surface (Fig. 1). Resistance of the bolometer at room temperature was 30 ohm. A YAG:Nd^{3+} laser was used as the radiation source; in the pulse mode, pulse duration = 0.1 μsec, repetition rate = 100 Hz and maximum energy was 10^{-4} joules/pulse.

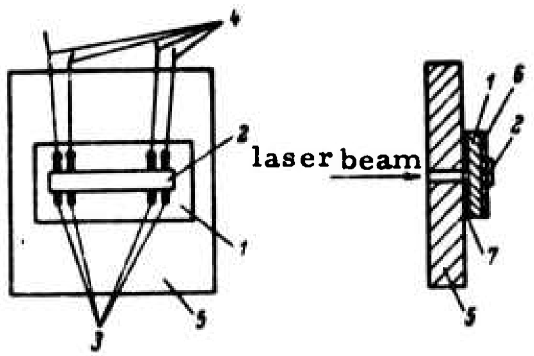

Fig. 1. Ge heating experiment.

1- Ge specimen; 2- superconducting Al bolometer; 3- Au contacts; 4- current and potential leads; 5- Cu heat sink (thickness 1 mm, surface area ~20 cm^2); 6- SiO layer (thickness 1000 Å); 7- cement.

In He^4 with the massive heat sink and pulsed irradiation, heatup of the target was not registered for pulse energies below 5×10^{-6} j, and did not exceed 0.13^{o} at 10^{-4} j pulses. In the latter case the heatup interval was not over 10 μsec. In He^3 both heatup level and duration were appreciably greater than in He^4.

Results for c-w exposure also showed heatup of only a fraction of a degree in both He^3 and He^4. At maximum excitation level (10^{-4} joules/pulse), overheating of Ge crystals attached to a heat sink with large surface and immersed in helium-4 at $T = 1.3^{o}K$ equals 0.13^{o} and overheating time $\tau = 10\,\mu$sec. Overheating effects are not detected at excitation level $E \leq 5 \times 10^{-6}$ joule/pulse during immersion of specimens in superfluid helium and helium-3 at $T = 1.3^{o}$ K. Experiments conducted in helium-3 show significantly high values of overheating and overheating time (up to 25 μsec). During continuous excitation of Ge, experimental values of ΔT agree well with calculations according to the formula for Kapitsa jump. For decreasing deviation of specimen temperature from that of the helium tank it is necessary use a massive heat sink with a larger surface and possibly thinner specimens.

Volod'kina, V. L., and V. L. Komolov. <u>Kinetics of the thermal breakdown of semiconductors under the action of light.</u> ZhTF, no. 1, 1975, 134-135.

The present work attempts to find solutions to two important problems: (1) To determine threshold breakdown value of a semiconductor under known conditions of heat transfer, and (2) To find the breakdown time of a crystal for a given intensity of light above the threshold breakdown value. The problem is discussed for the case in which absorption of light in the semiconductor with frequency $\omega < E_g/\hbar$ (E_g - forbidden zone width) is due to carriers in the conductivity zone. Results are described of the analysis of nonstationary thermal breakdown in a semiconductor plate under the action of intensive light flux. An expression is developed for the breakdown

development time at over-threshold light intensities. It is shown that in the limiting case of nearly adiabatic conditions, breakdown development time is determined by light intensity alone.

Experiments were conducted for investigating thermal breakdown using a CO_2 laser, operating c-w with maximum power up to 50 watts. Specimens used were Ge plates (ρ = 40 ohm x cm). The experimental value for threshold breakdown of a plate of 1.4 mm thickness was 20 w/cm^2, which agrees well with calculations. The time interval during which the absorption increased by a factor of two owing to a flux density of 21 w/cm^2, was 0.8 sec, while the calculated value was 0.17 sec. This discrepancy, according to the authors, can be ascribed to the geometry of the experiment and to the small dimensions of the laser beam.

4. Miscellaneous Studies

Askar'yan, G. A., and N. M. Tarasova. Passage of accelerated particles and quanta through a medium along a channel of reduced density produced by a laser beam. ZhETF P, v. 20, no. 4, 1974, 277-280.

The authors show experimentally and theoretically that ionization and heating of a medium by laser beam can create a channel of reduced density, through which accelerated particles (charges, quanta, macrons) and beams can pass with minimal scattering and energy dissipation.

Experiments were conducted as shown in Fig. 1. A Q-switched

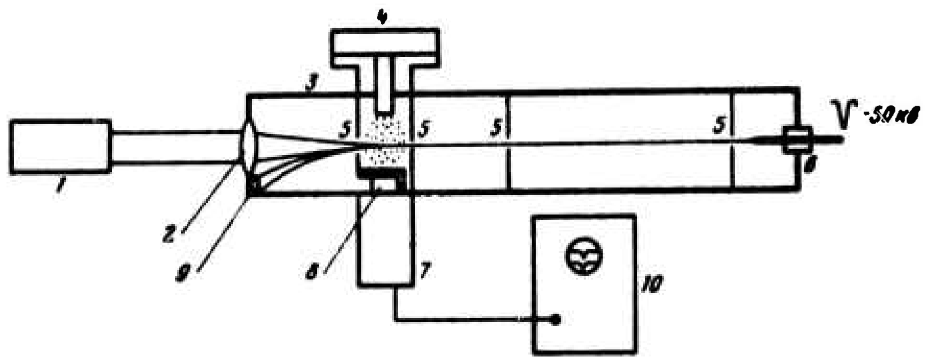

Fig. 1. Experimental arrangement

1- Nd laser; 2- lens (f = 8 cm); 3- vacuum chamber; 4- high-speed valve; 5- diaphragm; 6- needle cathode; 7- photomultiplier; 8- scintillator; 9- target; 10- oscillograph.

Nd laser was used with pulse duration of 30 nsec and energy up to 3 joules, focused on the gas cloud admitted by valve 4. An electron pulse from needle cathode 6 was triggered by the laser, with current through the optical spark region being deflected to Pb target 9; x-radiation from the target was used to evaluate the transit current. Results showed a sharp increase in current through the spark region; the gating effect persisted up to several hundred microseconds after the laser pulse.

It is noted that instead of a laser beam, millimeter beams in the SHF range could also be used for creating a low-density channel in a medium, although their directivity is poor compared to light beams.

Lokhov, Yu. N., V. S. Mospanov, and Yu. D. Fiveyskiy. Optical distortions in lenses from thermal effects of a powerful laser pulse. FiKhOM, no. 4, 1974, 28-31.

The mechanism of "thermal lens" formation (slight changes in refraction index of a lens when heated) caused by a powerful Gaussian laser pulse of millisecond duration is analyzed, taking into account surface and internal absorption. Effects of various factors (normal and radial temperature gradients, surface deformation, pressure, etc.) are estimated in the process of thermal distortion formation in a lens.

The authors conclude that in design of a high-powered laser system with millisecond pulses, it is necessary to determine the critical value of energy density in the laser pulse ϵ_m, at which the relative change in radiation intensity η due to thermal distortions of the focusing optics does not exceed a tolerable limit. A formula is derived for calculating ϵ_m. In a given example, for an optical glass lens of thickness $\ell = 1$ cm and focal length $f_o = 10$ cm, focusing a millisecond Nd^{3+} laser pulse with beam radius $a = 1$ mm; $\lambda = 10^{-4}$ cm; $\alpha_s = \gamma\ell = 10^{-3}$, ($\gamma$ - coefficient of internal absorption) and $\eta = 1$, the value of ϵ_m is about 600 joules/cm^2, which is significantly lower than the damage threshold for this case. Reduction of radiation intensity in the focal region in this case was by a factor of 2.

Bykovskiy, Yu. A., A. G. Dudoladov, V. P. Kozlenkov, and P. A. Leont'yev. Oriented crystallization of laser-produced thin films. ZhETF P, v. 20, no. 5, 1974, 304-307.

Structures of thin films, deposited by means of a Q-switched laser, were experimentally investigated. The target material used was Bi_2Te_3, with NaCl and mica plates used as substrates. Temperature of the substrate was varied from 20 to 350° C. Energy flux density at the target surface was $\approx 10^9$ w/cm^2; vacuum pressure was held at 10^{-5} torr. Distance between the substrate and target was 25 mm. The thickness of film deposited per radiation pulse was a few hundreds of an angstrom. Deposited films were separated from their substrates and were studied by an electron diffraction method using an EG-100A camera.

Electron diffraction patterns (6 photos are given) of thin Bi_2Te_3 films deposited on NaCl and mica showed that the films have different structures and orientations depending on temperature. The structure and orientation improved with increase in substrate temperature. Results show that orientation occurs only at the moment of material condensation.

Heating of the substrate up to 250° C yields an epitaxial Bi_2Te_3 film, whose basal plane of the hexagonal lattice is oriented parallel to the substrate. Epitaxial films of improved forms were also obtained at temperature $\approx$ 350° C. In certain cases, films were obtained with only a type [10.5] orientation in the 300-350° C temperature range.

The experiment shows that it is possible to control or regulate the degree of structural perfection of deposited films even at condensation rates up to 10^{10} Å/sec.

Alexandrescu, R., E. Cojocaru, and V. G. Velculescu. Nonlinear thermal effects from laser irradiation. Rev. roum. phys., v. 19, no. 2, 1974, 167-176. (RZhF, 9/74, #9Ye977). (Translation)

The temperature distribution in iron was calculated at the center and at varying distances from the laser heating spot at different increments of time, assuming a dependence of thermal conductivity coefficient k on temperature, as well as k = constant = 0.19 cal/cm/sec/^{o}C. Calculations were conducted for a cylindrical body of finite thickness under irradiation by a flux of 960 cal/cm^2/sec, distributed over the spot uniformly or with a Gaussian distribution. It is shown that neglecting the actual values of k cannot be compensated sufficiently accurately by using its average values alone.

Alexandrescu, R., E. Cojocaru, and V. Velculescu. Using the method of finite differences for calculating temperature distribution from laser irradiation. Stud. si cerc. fiz., v. 26, no. 2, 1974, 239-245. (RZhRadiot, 8/74, #8Ye248). (Translation)

[Beam-target] calculations were done by the Krenk-Nicholson method, which accounts for a series of effects that are usually neglected, including effects of the shape of irradiated body, thermal losses, and others. Temperature distribution curves are drawn for bodies of different shapes (plate, cylinder), and comparisons are made for Gaussian beams vs. beams with circular cross-section.

Strekalov, V. N. Application of the variational principle to the solution of kinetic equations. FTT, no. 1, 1975, 161-165. (Translation)

Possibilities are discussed of solving the quantum kinetic equation for electrons of a crystal in the electric field of light waves, by use of the variational principle. Conditions are obtained for applying the usual variational method to such a problem, which uses self-conjugate scattering operators. It is shown that in the case of self-conjugate operators it is not possible to obtain a meaningful physical result for medium-energy electrons. Use of another variational method,namely the method of least squares, allows one to determine the relationship of electron temperature to light intensity.

Mukhamedgaliyeva, A. F., A. M. Bondar', T. A. Ziborova, R. I. Baranov, and M. I. Panin. Study of the effect of free-running CO_2 laser radiation on minerals of the quartz group and quartz- containing rocks. Kvantovaya elektronika, no. 1, 1975, 37-42.

Beam-target experiments were conducted on specimens of minerals and rocks with volumes of 20-100 cm^3, using a CO_2 laser with a power density of 10^5 w/cm^2 and $\lambda = 10.6\mu$. Irradiation time was 30-60 sec. Target specimens are listed as gas-free rock crystal, rose-orange opal, sandstone, quartzite and agate.

An analysis of test results shows that heating during irradiation occurs basically on account of direct radiation absorption by Si-O stretching vibrations (800-1350 cm^{-1}), rather than because of structural defects. The breakdown is associated either with a sharp increase of thermal expansion

in the phase transition region which results in thermal stresses (brittle fracture), or with low-temperature thermal decomposition and silica evaporation with subsequent formation of a high-temperature flare and melt zone.

Smilga, V. I., T. D. Fetisova, G. R. Levinson, and I. G. Stoyanova. Change in optical properties of thin resistive layers under the action of laser radiation. IAN Fiz, no. 11, 1974, 2322-2327.

Results are described of a study of the generation mechanism of openings in thin resistive films based on CrSiO cermet, caused by laser radiation. The parameters of the nitrogen laser used were: λ = 337 nm, pulse power = 10^4 w, pulse duration, 8 nsec. The film thickness was 24-48 nm, surface resistivity 0.5-2.5 kOhm/square. The films were deposited on a quartz substrate.

The measured distributions of optical density in the films are shown in Fig. 1. Fig. 2 shows the dependences of film absorption capacity on the number of laser shots. A microscopic examination reveals three phases in the interaction process: 1) Cr_3 Si crystals are formed in the center of the irradiated region (D increases); 2) partially melted granules of Cr_3 Si are formed and material continuity is disturbed (D decreases); 3) Cr_3 Si granules migrate in the direction of temperature gradient over the film and fissures are formed.

The threshold intensity calculated for the model described, using thermophysical constants for 70 Cr-30 SiO, was found to be $q^* = 8.4 \times 10^6$ w/cm^2, while the experimental value was 7.0×10^6 w/cm^2. The dependence of

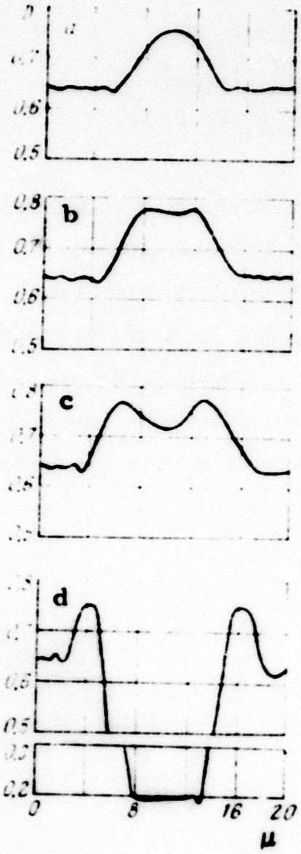

Fig. 1. Distributions of optical density in thin films (ρ = 2.5 kOhm/sq., q_0 = 5.5 x 10^6 w/cm^2, λ = 365 nm) in the case of one (a), two (b), four (c), and sixteen (d) irradiations.

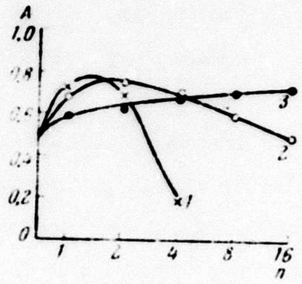

Fig. 2. Dependences of absorption capacity of a thin film on the number of laser pulses at different power density: 1- 7.1 x 10^6; 2- 5.5 x 10^6; 3- 4.4 x 10^6 w/cm^2.

threshold intensity on film transparency calculated for the same model is also shown graphically. It agrees with experiments which give threshold intensity = 6.0-8.0 x 10^6 w/cm^2 for all films. The absorption capacity of thin resistive layers exposed to laser irradiation is seen to increase by a factor of 2 to 4.

Kozlov, B. M., B. B. Krynetskiy, and A. A. Samokhin. Evaporation of a metastable liquid. Kvantovaya elektronika, no. 11, 1974, 2348-2352.

Characteristics of the explosive breakdown of a superheated metastable liquid in the presence of a free interface are discussed. It is shown that a pulsating regime of evaporation of an absorbing material can appear under laser irradiation, without substantial shielding of the incident radiation by the ejected surface layer of the liquid. If the duration of radiation absorption exceeds the characteristic time of the nonstationary thermal effect of the interface, then upon reaching the limit of overheating, in some cases, the explosive breakup of a metastable liquid can have a fine structure characterized by high-frequency pulsations ($\leq 10^{-5}$ sec).

Similar pulsating evaporation should be observed as well during the type of explosive decay induced by a sudden drop of the pressure at the surface of a metastable liquid previously heated to a temperature of $0.9\ T_c \leq T \leq T_C$ under equilibrium conditions.

Grachev, Yu. N., and G. M. Strelkov. Convective evaporation of a water droplet in a radiation field. Kvantovaya elektronika, no. 10, 1974, 2192-2196.

Convective evaporation of a water drop in an intense laser field with wavelength = 10.6 μ is theoretically considered. A system of integro-differential equations describing the process of drop evaporation was obtained in a quasistationary approximation. Time dependences of drop radius as well as temperatures at the surface and in the center of a drop during the entire evaporation process were determined and plotted. The upper and lower limits of the convective regime for drops with different initial radius R_o were found. At $R_o = 10\ \mu$ the temperature of explosive boiling is reached at a radiation power density of 1.3×10^4 w/cm^2.

Afanas'yev, Yu. V., and O. N. Krokhin.
High-temperature and plasma effects of high-power laser radiation interaction with matter.
IN: Sb. Fizika vysokikh plotnostey energii.
Moskva, Izd-vo Mir, 1974, 311-353. (RZhF, 10/74, no. 10G338). (Translation)

Laser radiation effects on opaque condensed materials are studied theoretically within a wide range of flux densities. This extensive study shows that the heat equation and vaporization kinetics theory do approximate fairly well the actual processes, but only within a relatively narrow range of flux densities well below 10^5 to 10^6 w/cm^2. At higher flux density of incident radiation, a gas dynamic approach to the problem is required. Although the physical problem of the interaction mode is clear enough, a thorough study of the interaction problem is possible only by common numerical solution of gas dynamic equations, together with the heat and radiation transfer equations.

5. Laser-Plasma Interaction

Afanas'yev, Yu. V., N. G. Basov, P. P. Volosevich, Ye. G. Gamaliy, et al. Laser initiation of thermonuclear reactions in inhomogeneous spherical targets. ZhETF P, v. 21, no. 2, 1975, 150-155.

A new laser CTR system is proposed, which is based on using laser pulses of simple form and inhomogeneous shell targets with a large mass of thermonuclear fuel, i.e. 10^2 times greater than masses cited in previous works. The main idea behind the suggested scheme is connected with the development of a compression mode in hollow spherical shells having a high value of radius to thickness ratio $R/\Delta R = 10^2$. In such targets it is possible to compress masses of 10^{-3} - 10^{-2} g up to densities $\sim 10^2$ g/cm^3 with a simple form of laser pulse at energies $E_L = 10^5$ - 10^6 joules. During the action of a laser pulse on such a target with pulse duration less than the time of material collapse at the center, compression occurs at mass slowdown near the center. These conditions enable one to determine target dimensions and pulse duration for a given value of laser energy.

Calculations are presented for laser energy $E_L = 10^6$ joules and the following characteristic values: radius R = 1 cm, laser pulse duration $\tau = 10^{-7}$ sec, mass of fuel = 10^{-2} g, density = 10^2 g/cm^3, $R/\Delta R = 10^2$. The portion of incident radiation energy transmitted to the energy of compressible material in this case would be n = 20% (hydrodynamic efficiency), which is sufficient for thermonuclear burn.

The possibilities of realizing the cited scheme are theoretically discussed. Calculations are made for different D-T target masses at laser energy $E_L = 10^6$ joules (Table 1). It is seen from the results that an energy gain amplification of $\sim 10^3$ is possible for laser energy $E_L = 10^6$ joules. The

$E_0 = 10^6$ j

Mass of DT, g	R, cm	Pulse duration, sec	Transmission coefficient, η,%	Density g/cm^3		Temperature, kev		Amplification factor E_T/E_L
				center	average	center	average	
10^{-3}	0,3	$1{,}5 \cdot 10^{-8}$	9	30	960	21	0,65	122
$2 \cdot 10^{-3}$	0,3	$1{,}5 \cdot 10^{-8}$	11	20	140	14	0,4	160 ÷ 320
$1{,}5 \cdot 10^{-2}$	1	10^{-7}	20	1	100	6	0,04	10^3
			$E_0 = 10^5$ j					
$6 \cdot 10^{-5}$	0,1	$3 \cdot 10^{-9}$	8	46	1100	10	0,54	110
			$E_0 = 10^4$ j					
$6 \cdot 10^{-6}$	0,05	$2 \cdot 10^{-9}$	8,5	54	1160	18	0,55	80

Table 1

authors conclude that the suggested laser-target system can lead to a new approach in development of the same for obtaining a closed energetic cycle in a laser thermonuclear reactor. The concept could also be useful for other pulsed thermonuclear devices, such as initiation of thermonuclear reaction by electron beams.

Basov, N. G., Yu. A. Zakharenkov, O. N. Krokhin, Yu. A. Mikhaylov, G. V. Sklizkov, and S. I. Fedotov. Generation of D-T neutrons during spherical heating of a solid target by high power laser radiation. Kvantovaya elektronika, no. 9, 1974, 2069-2071.

Studies are described of highly energetic components of neutron radiation from a laser plasma. The experimental technique used the nine-beam irradiation system reported earlier by Basov et al. (cf High Power Lasers, no. 2, Jan. 1973, 12).

In addition to 2.45 Mev neutrons, more energetic neutrons were also recorded in the present series of experiments. The transit-time measurement of energy led to the conclusion that they were generated from the $D(t, n)He^4$ reaction (neutron energy ≈ 14 Mev). Fig. 1 shows a characteristic oscillogram of neutron radiation from the plasma for the case of D-T

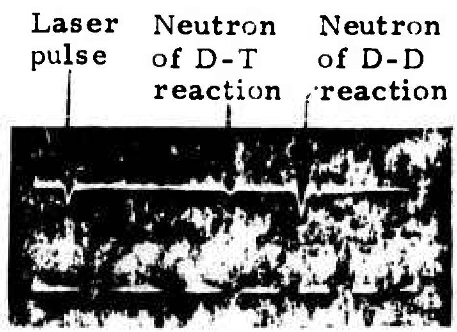

Fig. 1. Oscillogram of D-T neutron recording.

neutrons recorded during irradiation of a $(CD_2)n$ target of 160 μ diameter by a laser with pulse duration of 2 nsec and energy of 350 joules. It was found that the time interval between D-D and D-T pulses, $\Delta \tau = 24$ nsec, at a distance from target to counter $L = 0.9$ m, corresponded to the energy difference between the two types of neutrons.

D-T neutron yields during spherical heating of the target are estimated, and a relation is found between the yield of D-T and D-D neutrons. The authors note that the quantitative measurement of D-T neutron yield from a laser plasma for the case of a compressed hot nucleus ($T \geq 1$ kev) can be used for determining the degree of compression. In conclusion, they note that an interesting possibility exists for analysing target compression based on the products of thermonuclear reaction by recording protons, generated in the reaction $D(He^3, p)He^4$ where $E_p = 14.67$ Mev). The source of He^3 nuclei in this case is the $D(d, n)He^3$ reaction ($E_{He^3} \cong$ 0.82 Mev).

Basov, N. G., O. N. Krokhin, G. V. Sklizkov, and S. I. Fedotov. <u>Plasma heating and neutron generation during spherical irradiation of a target by high-powered laser radiation.</u> Lazery i ikh primeneniye. Trudy FIAN, v. 76, 1974, 146-185. (Translation)

A description is given of a high-powered laser device with a series-parallel amplifier system for high-temperature heating of plasma. The main output parameters are experimentally investigated, and coherent properties and spectral components are studied. Radiation energy at a pulse duration of 1 to 16 nsec equals 400-1300 joules, degree of contrast $\approx 10^7$ and luminance $\approx 10^{17}$ watt/cm^2/ster. Requirements are analyzed for a laser system intended for high-temperature heating of a plasma during spherical irradiation of a target, and for realizing practically attainable thermonuclear reactions.

Processes taking place during high-temperature plasma heating from spherical irradiation of an isolated solid target by a nine-beam laser were experimentally studied. X-radiation from the plasma was investigated, and it was found that in this spectral region, 20% of the total energy absorbed by laser radiation plasma is converted into x-rays. Neutron yield from a (CD)n plasma was recorded and attained about 10^7 neutrons/pulse. It is shown that generation of neutrons in a laser plasma during spherical irradiation has a thermal character. Gasdynamic processes of plasma expansion are analyzed. Pressure on the target surface owing to ablation reaches a value 2×10^8 bar. It is shown that at such pressures, strong compression occurs of the plasma nucleus up to a value $\cong$ 40.

Krokhin O. N., Yu. A. Mikhaylov, V. V. Pustovalov, A. A. Rupasov, V. P. Silin, G. V. Sklizkov, and A. S. Shikanov. Anisotropy of x-radiation from a laser plasma. ZhETF P, v. 20, no. 4, 1974, 239-243.

The authors describe a rigorous study on the angular distribution of x-radiation from a dense laser plasma, generated by focusing a polarized Nd glass laser (λ = 1.06 μ) on the surface of an aluminum target. The aim was to evaluate anisotropy of x-ray emission, believed to be a result of parametric instability development.

The experimental sketch is shown in Fig. 1. Laser parameters were: energy up to 30 joules, duration = 3.5 nsec, contrast not less than 5×10^5 and divergence = 5×10^{-4} rad. Polarized laser radiation (polarization level ~ 90%) was focused with a lens of f = 10 cm; incident flux density q $\cong 10^{14}$ w/cm^2. Angular distribution of x-ray quanta in the energy range of 1.3-12 kev was investigated. X-ray photofilms with sensitivity to 1Å were used as detectors; these were placed in special cassettes having 14 beryllium input

filters of thickness 100-2600 μ. The cassette detectors were placed at different angles to the investigated plasma and to the polarization vector E, as shown in Fig. 1.

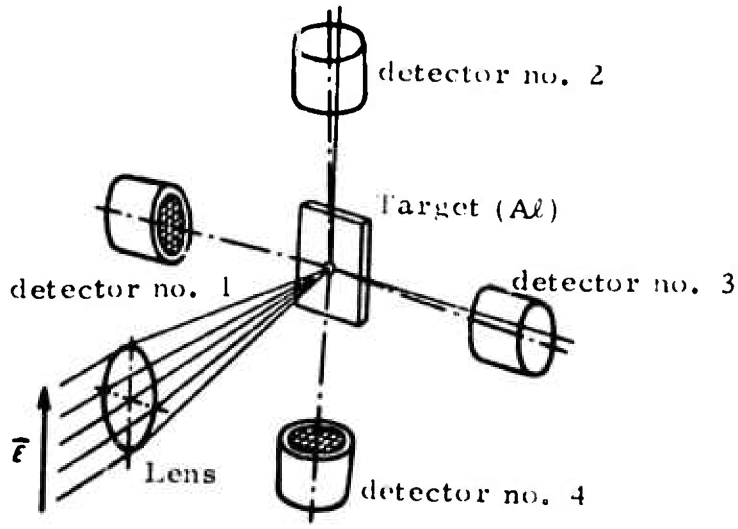

Fig. 1. X-ray anisotropy experiment.

A significant anisotropy was detected at flux densities above 3×10^3 w/cm^2. This conclusion was based on the fact that the number of x-ray quanta per unit solid angle emitted in the direction normal to $\bar{E}$ was much greater than those emitted parallel to $\bar{E}$. Fig. 2 shows results of the measurement of anisotropy degree ζ, determined as a ratio between number of per-unit x-ray quanta normal to $\bar{E}$ and parallel to $\bar{E}$, as a function of limiting transmission energy of the beryllium filters, E_{lim}. Electron temperature T of the plasma was also measured in the experiment and was found to be also anisotropic. Electron temperature measured normal to $\bar{E}$ was $\sim$350 ev, while the temperature for the parallel direction was 700 ev.

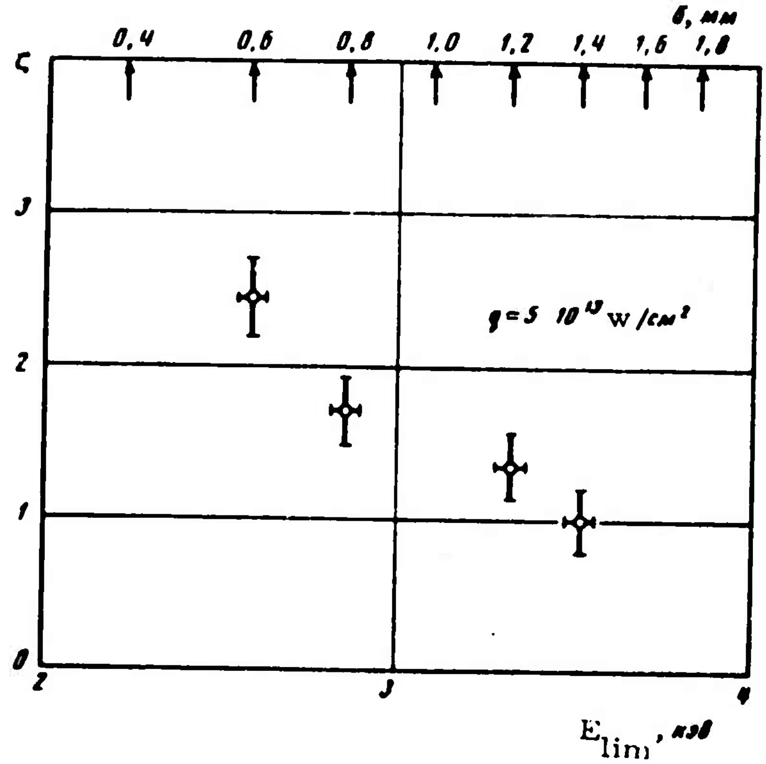

Fig. 2. Degree of anisotropy ζ of x-radiation as a function of limiting transmission energy of beryllium filter, E_{lim} (kev).

Aglitskiy, Ye. V., V. A. Boyko, S. M. Zakharov, S. A. Pikuz and A. Ya. Fayenov. Observation in a laser plasma and identification of dielectron satellites of the spectral lines of H- and He-like ions of elements in the Na--V interval. Kvantovaya elektronika, no. 4, 1974, 908-936.

Observations of spectral lines of H- and He-like ions of Na, Mg, Al, Si, P, S, Cl, K, Ca, Ti, and V (Z = 11--23, ionization potential to 6.86 kev) are described, occurring in a laser plasma. The tests also identified the transitions $n\ell n'\ell'$ - $1sn'\ell'$ and $1s2pn\ell$ - $1s^2n\ell$ of He- and Li-like ions, respectively. The experimental sketch is shown in Fig. 1.

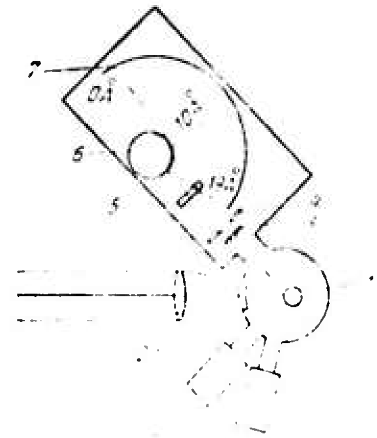

Fig. 1. Test arrangement

1- target; 2- two-component objective (f = 7.5 cm); 3- filter (5μm Dacron, 0.1μm Aℓ); 4- limiting diaphragm; 5- opening for dividing tracks in photographing several spectra; 6- mica crystal; 7- photofilm; 8- continuous x-ray recording channels.

The plasma was heated by 50 j laser pulses of 1.8 ns duration and divergence not less than 3×10^{-4} rad. Radiation was focused with a two-component objective into a spot of diameter 80 μ on the target surface; flux density reached 5×10^{14} w/cm^2.

The spectrograph used has a convex mica crystal, allowing spectral registry in the 0.5 - 19 Å range. The angle between the incident laser radiation and the spectrograph axis was 60°; spectra were recorded on special films. Target specimens used were NaCℓ, Mg, Aℓ, SiO_2, P, S, KCℓ, CaO, Ti and V. Experimental results are tabulated together with those of other workers. The number of lines measured and identified totalled 180; accuracy in measuring wavelengths equalled 0.002 Å for λ = 10 Å and 0.005 Å for λ = 2.5 Å.

The obtained results are considered of interest in diagnostics of a dense laser plasma. In previous works, electron density measured according to lines of He-like ions with Z = 6 was $N_e = 10^{16}$ cm^{-3}, and with ions Z = 12 in the case of a laser plasma,was $N_e = 10^{20}$ cm^{-3}. The authors point out that by using an ion with higher Z, one could in principle obtain a measurement of electron density in the range of $N_e = 10^{23}$ cm^{-3}.

Aglitskiy, Ye. V., V. A. Boyko, S. A. Pikuz, and A. Ya. Fayenov. Identifying the spectra of lithium-like ions of Ti, V and Cr contained in a laser plasma in the 8.5--17 Å range. Kvantovaya elektronika, no. 8, 1974, 1731-1741.

This paper gives a detailed report on lithium-like ion spectra of Ti, V, and Cr, formed during sharp focusing of powerful laser radiation on a solid target in vacuum. A large number of spectral lines, corresponding to transitions from higher levels (n = 4 to 9) were observed. Wavelengths of $3 \rightarrow 2$ transitions were measured with more accuracy than in cited previous work, and were resolved closer to the line locations $^2P_{3/2}$ - $^2D_{5/2}$, $^2P_{3/2}$ - $^2D_{3/2}$. The presence of high-level transitions permits experimental determination of the ionization potentials TiXX, VXXI, and CrXXII. Comparison of the measured wavelengths with those of theoretical calculations suggests the possibility of using calculated data for elements with still higher Z (e.g FeXXIV, CoXXV, etc).

Fig. 1 gives the spectrograms of the laser plasma emission

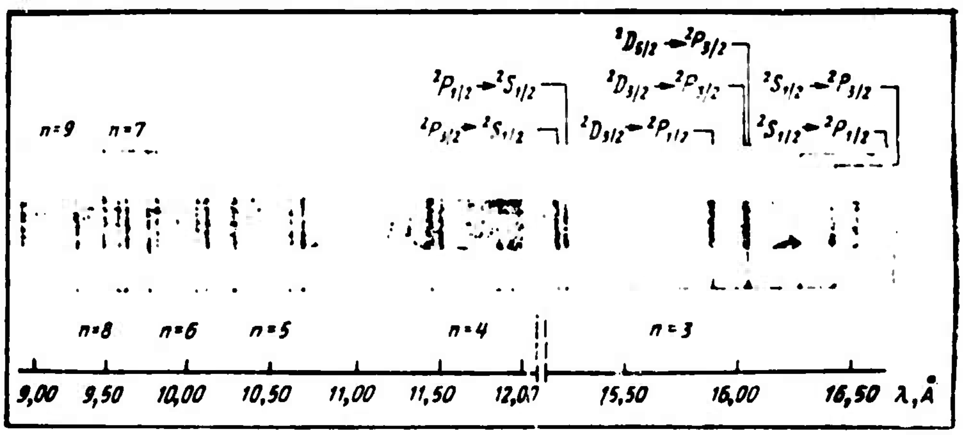

Fig. 1. Spectrogram of laser plasma emission containing TiXX ions.

containing TiXX ions. Plasma heating was done with a neodymium laser at a pulse energy ~ 50 joule and nominal duration of 2 nsec. The spectrograph

used had a convex mica crystal (0.5 Å ≤ λ ≤ 19.5 Å), which permitted recordings in the more shortwave regions. Spectrograms of the laser flare were obtained on type UF-VR films for 10-15 flashes.

Tabulated data are included comparing the observed transitions with those previously reported in the literature.

Aglitskiy, Ye. V., V. A. Boyko, O. N. Krokhin, S. A. Pikuz, and A. Ya. Fayenov. Observation of ions with charge = 30 to 50 in a laser plasma. Kvantovaya elektronika, no. 9, 1974, 2067-2069.

The presence of ions with Zof 30 to 50 ($A/Z \sim 3$, A-atomic weight) was recorded by means of x-ray spectroscopy in a laser plasma, with charge significantly exceeding those obtained in earlier studies. ($Z \gtrsim$ 20--25). Experiments were done with a laser (unspecified) which with sharp focusing achieved a flux density of 5×10^{14} w/cm. The radiation spectrum of the plasma in the range of 0.1--2 nm was recorded similarly to the method reported previously by the authors (cf. Kvantovaya elektronika, 1, 908, 1974).

In highly-ionized spectra of Y, Zr, Nb and Mo, brighter lines were noted in transitions of Ne-like ions. Table 1 shows the calculated values of ionization potential together with relative intensities and identification of transitions $2s^2 2p^6$ - $2s^2 2p^5 3s$, $2s^2 2p^5 3d$, $2s 2p^6 3p$, which were detected on the basis of precise wavelengths of Ni^{18+}, Cu^{19+}, Zn^{20+}, subsequent interpretation of the obtained Ge^{22+} and Se^{24+} spectra, and extrapolation to higher levels of Z. Values of A/Z for ions observed in the present experiment

Table 1

Transitions	Y^{29+}		Zr^{30+}		Nb^{31+}		Mo^{32+}	
	I, rel. un.	λ, nm	*I*, rel. un.	λ, nm	*I*, rel. un.	λ, nm	*I*, rel. un.	λ, nm
$2s^22p^6\ {}^1S_0 - 2p^53s\ {}^3P_1$	9	0,6196	9	0,5831	9	0,5502	9	0,5202
$2s^22p^6\ {}^1S_0 - 2p^53s\ {}^1P_1$	6	0,5966	6	0,5609	6	0,5278	6	0,4980
$2s^22p^6\ {}^1S_0 - 2p^53d\ {}^3D_1$	10	0,5709	10	0,5373	10	0,5077	10	0,4804
$2s^22p^6\ {}^1S_0 - 2p^53d\ {}^1P_1$	8	0,5527	8	0,5198	8	0,4903	8	0,4630
$2s^22p^6\ {}^1S_0 - 2s2p^63p\ {}^3P_1$	3	0,5299	3	0,4997	3	0,4721	3	0,4464
$2s^22p^6\ {}^1S_0 - 2s2p^63p\ {}^1P_1$	2	0,5251	2	0,4950	2	0,4674	2	0,4416
E, kev	3,559		3,829		4,067		4,312	

are: $Y39^{29+}$ - 3.07; $Zr40^{30+}$ - 3.03; $Nb41^{31+}$ - 3.00; $Mo42^{32+}$ - 3.00; $Ta181^{48+}$ --$Ta181^{54+}$ - 3.36 - 3.77; $W182^{49+}$ --$W182^{55+}$ - 3.35--3.76. The overall number of ions in a single pulse, as calculated from spectral line intensity, attains 3×10^{11}, which is significantly higher than the values of 3×10^8 to 10^9, obtained for Ta and W at lower ionization levels in previous works.

Boyko, V. A., O. N. Krokhin, and G. V. Sklizkov. Investigating parameters and dynamics of laser plasma during sharp focusing of radiation on a solid target. Lazery i ikh primeneniye. Trudy FIAN, v. 76, 1974, 186-228.

This work gives an account of physical conditions occurring in a laser plasma subjected to radiation with flux density $q = 10^{10}$-10^{15} w/cm^2 and laser pulse duration of 10^{-11}-10^{-8} sec on a solid target in vacuum. Results are discussed of different experiments for determining maximum electron temperature of the plasma; electron density; life-time of ions in the hot nucleus of the laser flare; gasdynamic velocity of plasma dispersion; and maximum ionization level. These figures are respectively: T_e = (0.01-2.0) kev,

$N_e = 10^{20}$ cm^{-3}, $\tau = 10^{-9}$ sec, $v = 10^7$ cm/sec, and $Z = 20$. Based on these data, models are suggested for gasdynamic motion of the plasma and ionization equilibrium in the hot nucleus of the flare.

Anisimov, S. I., and N. A. Inogamov. Development of instability and loss of symmetry during isentropic compression of a spherical droplet. ZhETF P, v. 20, no. 3, 1974, 174-176.

The authors note that in symmetrical laser compression of spherical targets for CTR purposes, the ensuing motion instabilities which destroy target symmetry have not been adequately investigated.

A brief development is accordingly given of a general expression for distortion of an initial spheroid as a function of applied pressure and compression time. The model assumes the initial target shape to be ellipsoidal to a small degree, i.e. to have a deviation Δ_o from spherical << 1. It is then shown that for a degree of compression n, deviation from spherical will grow as $n^{1/2}$, for the isentropic compression case assumed. The solution places no constraints on the rate of the process or on constancy of pressure in the target mass.

Aglitskiy, Ye. V., V. A. Boyko, S. A. Pikuz, and A. Ya. Fayenov. Identification of Fe XXIV lines in the 6.5-11.5 Å range, observed in the spectrum of a laser plasma. (Fiz. in-t. ANSSSR. Lab. kvant. radiofiz. Preprint No. 56). M., 1974, 13 p.). (RZhF, 11/74, #11G70). (Translation)

A lithium-like spectrum of Fe XXIV obtained by focusing powerful laser radiation into a solid target in vacuum was studied. A neodymium laser with pulse energy of 50 j and duration≈2 picosec was used.

The spectrum of highly ionized Fe in the 6.5-19.5 Å range was obtained by means of a spectrograph with convex mica crystal. Wavelengths were determined from three reference points by means of a second order interpolation formula.

Kaliski, S. Laser compression of D-T with explosive precompression. Proc. Vibrat. Probl. Pol. Acad. Sci., v. 15, no. 1, 1974, 3-15. (RZhF, 11/74, #11G193). (Translation)

The possibility is evaluated for generating a laser plasma with a preliminary compression by an explosion. Rigorous solutions are obtained for plane waves and an approximate solution for spherical compressional waves. It is shown that lowering the critical power of value of the laser pulse is thus feasible.

Kas'yanov, Yu. S., V. V. Korobkin, P. P. Pashinin, A. M. Prokhorov, V. K. Chevokin, and M. Ya. Shchelev. Study of radiation of a laser plasma in the x-ray region. ZhETF P, v. 20, no. 11, 1974, 719-721.

X-radiation of a laser plasma with high spatial and time resolution was experimentally investigated. The experimental sketch is shown in Fig. 1. The radiation source was a neodymium laser consisting of a master oscillator and multistage amplifier. The oscillator worked in the regime of uniaxial and uniangular modes. R tangular pulses were generated with regulated durations in the 2-10 nsec range with rise time ~ 0.5 nsec. Energy output at pulse widths of 2 and 10 nsec was 30 and 60 joules respectively. Radiation was focused on a titanium target in a vacuum chamber by a lens of f = 10 cm. The diameter of the focal region

$\gtrsim 100\ \mu m$ and flux density on the target, - up to $2 \times 10^{14}\ w/cm^2$. X-radiation was studied by means of an electron-optical camera, consisting of a special scintillator with time resolution ~ 0.5 nsec, an image converter and control systems.

Along with the x-radiation of the plasma, studies were also conducted simultaneously of reflected laser radiation from the target, for which a second electron-optical camera was used.

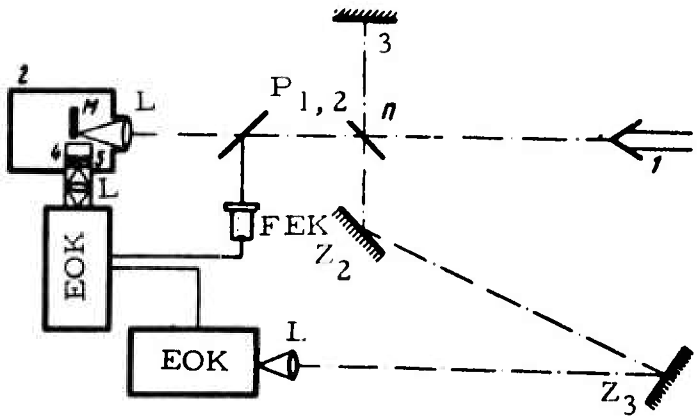

Fig. 1. Experimental sketch.

1- Laser beam; 2- vacuum chamber; 3- pinhole camera; 4- x-ray filter; 5- plastic scintillator; Z_{2-3}- mirrors; L- objectives; M- target; $P_{1,2}$- beam splitter; FEK- photoelement; EOK- electron-optical camera.

Typical experimental results are shown in Fig. 2. It is seen that in a smooth incident pulse, the reflected pulse has significantly high modulation. X-radiation of laser plasma also undergoes modulation in amplitude. Characteristic modulation period equals 1 ± 0.5 nsec and that of x-radiation, 0.7 ± 0.2 nsec. The presence of the x-radiation modulation indicates that a significant turbulence exists in the laser plasma. The characteristic modulation period coincides well with the time $\tau = a/v$, where a = characteristic plasma dimension, and v = ion sound velocity. In the present case at $T_e = 1$ kev, the time $\tau = 0.5$ nsec.

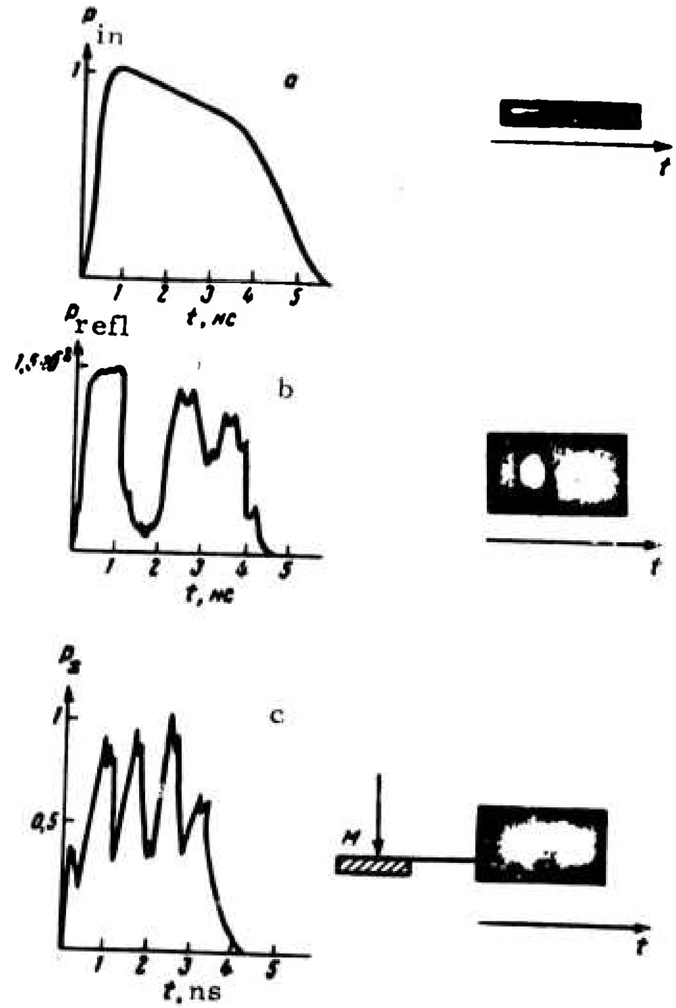

Fig. 2. Test results. a) incident laser radiation; b) reflected laser radiation from target; c) x-radiation.

Batanov, V. A., K. S. Gochelashvili, B. V. Yershov, A. V. Malkov, P. I. Kolisnichenko, A. M. Prokhorov, and V. E. Fedorov. <u>Generation of hard x-radiation of microsecond duration on a target during Q-switching of a laser by a plasma mirror.</u> ZhETF P, v. 20, no. 6, 1974, 411-416.

Generation of giant pulses of microsecond duration was experimentally observed from focusing of laser radiation in air or on solid

targets (graphite, deuterated polyethylene). Pulses were formed as a result of Q-switching of the laser by the plasma mirror formed. A neodymium laser with three-stage amplifier was used in the experiment, developing a directivity of 3×10^{-4} rad at up to 2 kj energy. It was operated in a millisecond pulsed regime with characteristic microsecond spiked modulations. Duration of giant pulses generated was 0.3 - 0.5 μsec (Fig. 1) and their energy reached 300 joules, which is about 30% of the total millisecond laser pulse energy.

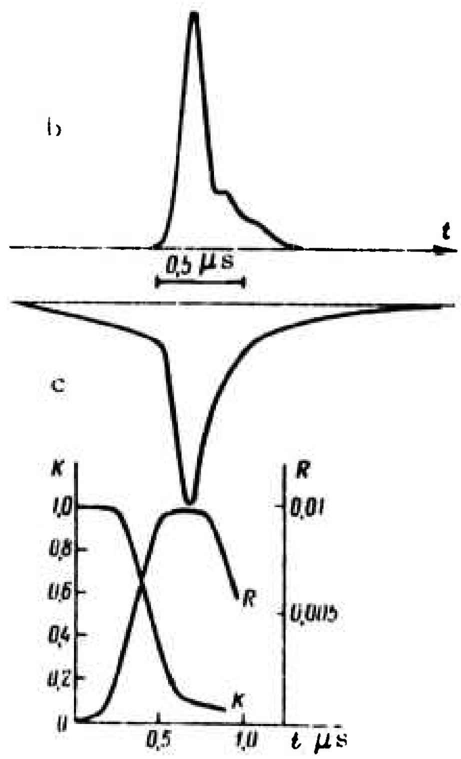

Fig. 1. Time structure of laser radiation pulses (a & b, lower); x-radiation of plasma (a & b, upper) for solid target (a) and air (b); time dependence of transmission K and reflection R of plasma in air (c).

When the laser was focused, a plasma was formed at first in the focal region. Then with increase in laser radiation intensity and generation of giant pulses owing to Q-switching by the plasma mirror, the plasma was heated to a high electron temperature: T_e 2-4 kev in air and T_e = 3-7 kev for solid targets. This gave rise to hard x-radiation (duration 0.1 μsec duration in air, 0.3-0.4 μsec in solids) which was recorded by a photomultiplier faced with a plastic scintillator and beryllium foils.

Reflection, transmission and the gasdynamics were investigated of the plasma generated in the laser focal region. The maximum value of reflection of the plasma mirror in air was R = 0.01 and that of its transmission, K = 0.1.

Bykovskiy, Yu. A., N. M. Vasil'yev, I. D. Laptev, and V. N. Nevolin. Study of neutral particles formed by the effect of laser radiation on a solid target. ZhTF, no. 12, 1974, 2623-2624.

Parameters of laser-produced hydrogen and deuterium atoms were measured by the method of mass spectroscopy. The targets of zirconium hydride and zirconium deuteride placed in a 5×10^{-6} torr vacuum were exposed to single-pulsed Nd glass laser radiation with pulse energy of 1 j and duration of 20 nsec. Focal spot radius was $\sim 200\ \mu$.

The measured values for velocity of hydrogen atoms are given in Fig. 1. Analogous results were obtained for deuterium atoms.

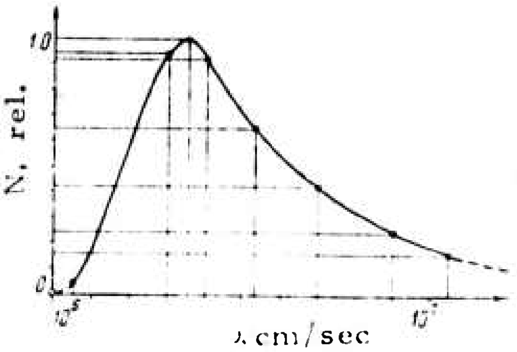

Fig. 1. Velocity distribution of hydrogen atoms.

The temperature of the hydrogen plasma was estimated to be about 5.6 ev (by the formula of Boyko et al., 1972). The number of deuterium and hydrogen atoms was calculated to be ~ 10^{16}, which correlates well with the total number of atoms evaporated from a solid target when exposed to a laser with the cited parameters.

It was concluded that the atoms detected in the experiments have recombination characteristics.

Boyko, V. A., O. N. Krokhin, S. A. Pikuz, and A. Ya. Fayenov. Measuring the radiation intensity of a laser plasma in the 2-10 Å range and determining electron temperatures for targets with nuclear charges of Z = 12-23. Kvantovaya elektronika, no. 10, 1974, 2178-2184.

Experiments were performed with a laser plasma produced by irradiation of deuterium-containing targets, both with and without an admixture of heavy elements. The parameters of the Nd laser used were: pulse energy 80 j, $\tau_{0.5}$ - 1.8 nsec, beam divergence 3×10^{-4} rad, and contrast 10^5. The diameter of the focal spot was 80μ, power density about 5×10^{14} w/cm^2. Laser plasma radiation in the 2-19 Å range was recorded by an x-ray spectrograph. The distance between the plasma and the film was 40 cm. Spectrographic dispersion ranged from 0.05 to 0.12 Å/mm; resolution was 0.002 Å.

The absolute intensity of the laser plasma radiation, in resonant lines of He-like ions per full solid angle, are given in Table 1.

The plasma electron temperatures determined from relative intensities of the resonant lines and their satellites are given in Table 2.

Table 1

Target	Ion	λ, Å	No. of laser shots	D	W, watts
Mg	MgXI	9.1682	1	0.7	6×10^7
Al	AlXII	7.7568	5	1.7	5.3×10^7
SiO_2	SiXIII	6.6488	9	0.5	2×10^6
P	PXIV	5.7591	12	1.6	2.7×10^7
S	SXV	5.0374	11	1.5	2.3×10^7
KCl	ClXVI	4.4438		0.5	5×10^5
	KSVII	3.5309	24	0.2	3.7×10^5
CaO	CaXIX	3.1766	24	0.2	4×10^5
Ti	TiXXI	2.6101	20	0.25	2×10^5
V	VXXII	2.3823	21	0.11	1.3×10^5

Table 2

Target	He-like ions			H-like ions		
	ion	E_i, keV	T_e^{sat}, eV	ion	E_i, keV	T_e^{sat}, eV
Mg	MgXI	1.762	230	MgXII	1.963	425
Aℓ	AℓXII	2.086	270	AℓXIII	2.304	550
Duralumin (93% Aℓ)	AℓXII	2.086	250	AℓXIII	2.304	600
SiO_2	SiXIII	2.433	360	SiXIV	2.673	500
P	PXIV	2.817	670	PXV	3.070	800
S	SXV	3.224	740	-	-	-
NaCℓ	CℓXVI	3.658	625	-	-	-
KCℓ	CℓXVI	3.658	560	-	-	-
	KXVIII	4.611	500	-	-	-
CaO	CaXIX	5.129	750	-	-	-
Ti	TiXXI	6.249	710	-	-	-
V	VXXII	6.851	800	-	-	-

The diameters of the luminescent regions are given in Table 3.

Table 3

Target	He-like ions			H-like ions		
	ion	ℓ, mm	T_e, ev	ion	ℓ, mm	T_e, ev
65% (CD_2)nt	MgXI	0.4	260	MgXII	0.2	450
+5% MgO + 30% P	PXIV	0.3	480	PXV	0.2	800
Mg	MgXI	0.6	250	MgXII	0.35	440
P	PXIV	0.4	540	PXV	0.25	750
T_i	T_iXXI	0.08	760	-	-	-

It was concluded that the possibility exists for determining the temperature distribution in a laser plasma based on the spectral intensities of ions with nuclear charges Z = 12-23.

Dubovoy, L. V., V. D. Dyatlov, V. I. Kryzhanovskiy, A. A. Mak, R. N. Medvedev, A. N. Popytayev, V. A. Serebryakov, V. N. Sizov, and A. D. Starikov. Study of a interaction of intense laser radiation with massive targets. ZhTF, no. 11, 1974, 2398-2403.

Beam-target experiments (see Fig. 1) were conducted using an Nd glass laser with pulse energy of 120 j and duration 9×10^{-11} sec focused on an LiD target in a vacuum at 10^{-5} torr. The beam divergence was 10^{-3} rad, focal spot = 200 μ, flux density at the target $= 10^{15}$ w/cm^2, and laser pulse contrast > 10^4.

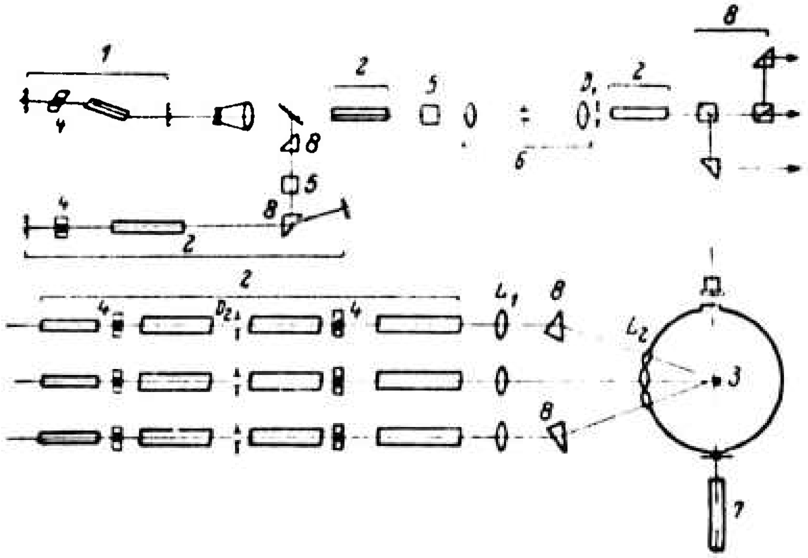

Fig. 1. Experimental set-up.

1- master oscillator; 2- amplifying stages; 3- target; 4- passive switches; 5- Pockels cells; 6- lens selector; 7- aligning He-Ne laser; 8- rotating prisms; L_1, L_2- focusing lenses; D_1, D_2- limiting apertures.

Electron temperature was measured to be 1-2 keV, and the x-ray energy was 100 mj. The maximum neutron yield was 6×10^5 n/4π. The experimental dependence of the neutron yield on applied energy is shown in Fig. 2, which also shows the dependence calculated by a formula developed by Plis et al., 1972. The experimental dependence of reflection index on the light flux intensity at the target is shown in Fig. 3. This dependence is suggested to indicate a nonlinear light absorption by the target. The existence of a nonlinear effect is also indicated by the appearance of second harmonics in the laser radiation, reflected at an angle of 162°. Although second harmonics were not detected in the laser radiation reflected at an angle of 135°, a large number of Li, D and admixture spectral lines were recorded at that angle.

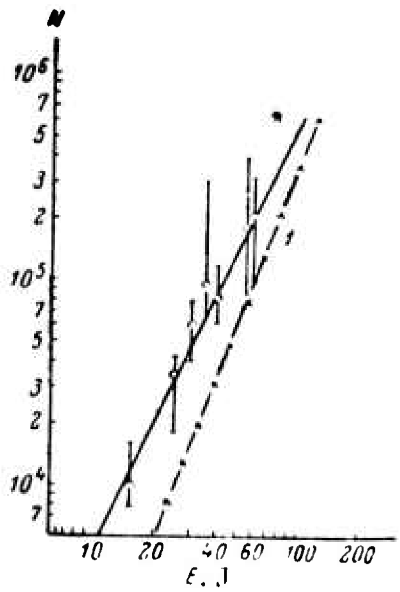

Fig. 2. Experimental (solid line) and calculated (broken line) dependence of neutron yield on incident energy.

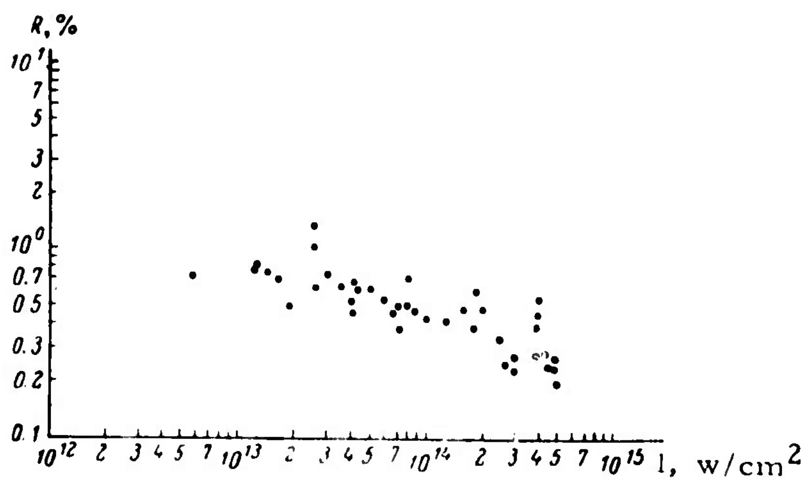

Fig. 3. Experimental dependence of reflection index $R = E_r/E_{in}$ on the intensity of incident light.

It was noted that the low R values measured can be attributed to a high contrast and the small pulse duration of the laser radiation. The rather high neutron yield confirms the conclusion as to the strong effect of laser radiation parameters on the interaction process. The article includes photos of the interaction process.

Gorokhov, A. A., V. D. Dyatlov, V. B. Ivanov, R. N. Medvedev, and A. D. Starikov. Some features of powerful laser radiation absorption during heating of a LiD target. ZhETF P, v. 21, no. 1, 1975, 62-65.

Various physical characteristics were experimentally studied of the initial stage of plasma heating during interaction of sub-nanosecond Nd laser radiation pulse with a LiD target, for flux intensities above 10^{16} w/cm^2. The basic laser system was that described in the foregoing article by Dubovoy et al. (ZhTF, no. 11, 1974, 2398). In the present tests radiation was focused on the polished target surface with objective f = 6 cm and relative aperture f/0.9. Uncertainty of target surface location relative to focal plane did not exceed 2 μm. Background radiations were measured by means of a calorimeter, photoelement and oscillograph. Contrast δ of the laser flare was found to vary from 10 to 5 x 10^4.

Dependence of flare dimensions and quantity of vapor products on contrast δ are determined. Maximum electron density along the optical axis, n_{emax}, and total number of evaporated particles from the target surface are found to increase with drop in δ. Fig. 1 shows the relationships of reflection coefficient R and maximum electron density as a function of δ. The dependence of the reflection coefficient on contrast is explained as the

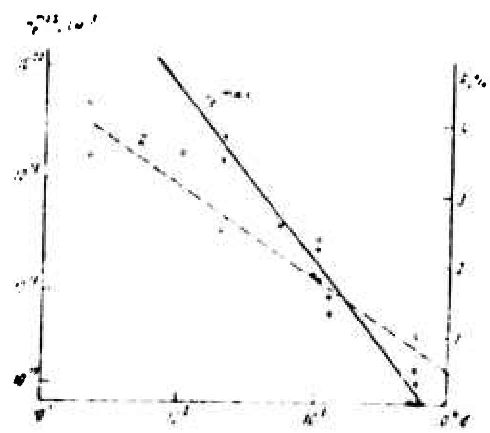

Fig. 1. Reflection coefficient R and maximum electron density n_{emax} as functions of contrast δ.

result of radiation defocusing during surface evaporation and changes in electron density. It is shown that in the intensity region $10^{15} \leq I \leq 3 \times 10^{16}$ w/cm^2, R monotonically decreases with increase of incident laser radiation.

Gorokhov, A. A., V. D. Dyatlov, R. N. Medvedev, A. D. Starikov, and V. G. Tuzov. Amplitude-spatial effects of transforming highly-intensive radiation in laser plasma. ZhETF P, v. 21, no. 2, 1975, 111-114.

This paper investigates certain effects causing spatial, amplitude and frequency variations of high-intensity laser radiation during its interaction with a dense plasma. Experiments were conducted with the laser system of Dubovoy et al. referred to in the previous two articles (ZhTF, no. 11, 1974). Additional recording systems were used for measuring angular distribution of reflected radiation near the pump frequency region ω_o and $2\omega_o$, as well as apparatus for localizing the maximum luminous region of the plasma at frequencies of ω_o, $3/2\ \omega_o$ and $2\omega_o$. Simultaneously with the measurements of spatial characteristics (angular distribution and transformation zone of incident radiation) in one of the harmonics, spectrographs were taken of this portion on an MDR-3 monochromator; incident and reflected spectra in the ω_o region were also recorded on a spectrograph with dispersion = 30.4Å/mm. Contrast, values of incident and reflected energy, and electron temperature of the plasma were regulated for each flare.

At intensities of 10^{15} - 3×10^{16} w/cm^2, radiation passed by the focusing lens contained frequencies $3/2\ \omega_o$, $2\omega_o$ and ω_o. The second harmonic $2\omega_o$ consisted of narrow and wide components, such that the energetic relationbetween the components was 2×10^{-3}. Correlation of the narrow component with incident radiation intensity was very weak, while that of the wide components equalled $I(2\omega_o) \sim I^{\alpha}(\omega_o)$ where $\alpha > 2$.

Maximum luminous plasma regions were localized at frequencies of $2\omega_0$ and $3/2\omega_0$; these regions were however not seen at ω_0. Discussions are given on different mechanisms which could account for the above observed effects.

Gamaliy, Ye. G., S. Yu. Gus'kov, O. N. Krokhin, and V. B. Rozanov. Possibility of measuring laser plasma characteristics from neutrons of a D-T reaction. ZhETF P, v. 21, no. 2, 1975, 156-160.

This is a study on the relationships of the characteristics of a laser plasma from a $(CD_2)n$ target with D-T reaction yield and a neutron spectrum formed. Two possible cases are studied: a) Compressed cold target nucleus, $T_e < 0.1$ kev (D-D reaction occurs only in the corona); and b) compressed hot target nucleus, $T_e > 0.3$ kev (D-D reaction occurs in corona and nucleus). Expressions are developed for the level of D-T neutron yield, Q_{DT}, and the energetic spectrum of D-T neutrons; dQ_{DT}/dE_n, where E_n = neutron energy). Ratios between the number of D-T and D-D neutrons formed in the plasma (Q_{DT}/Q_{DD}) are determined for both above cases, and results are plotted as a function of electron temperature T_e.

In the case of the hot nucleus, the ratio Q_{DT}/Q_{DD} is found to be significantly higher ($\gtrsim 10^{-3}$). The D-T neutron spectrum plotted for the hot nucleus as a function of tritium velocity v shows a horizontal portion on the top (Fig. 1); this is explained by the absence of tritium nuclei in that velocity range. The relationships of Q_{DT}/Q_{DD} and D-T neutron spectrum thus obtained permit the determination of the temperature and density of the cited plasma.

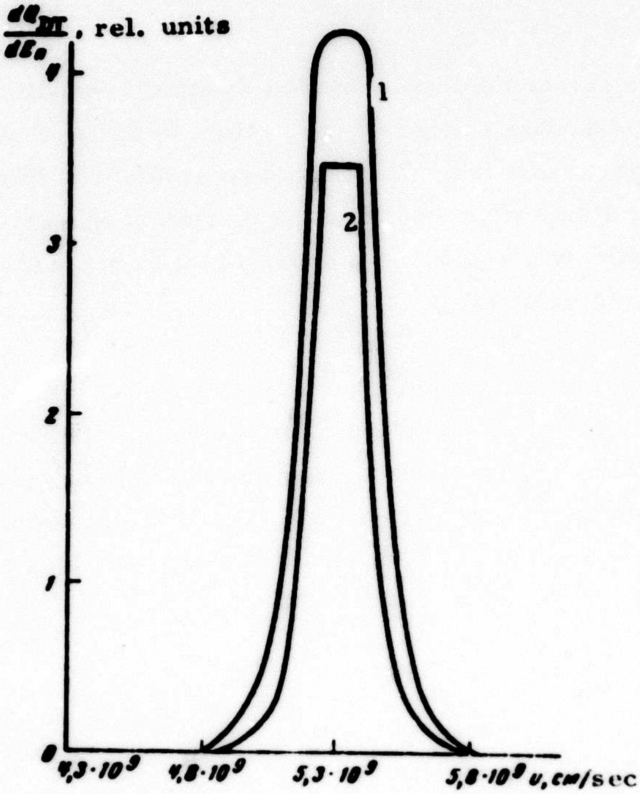

Fig. 1. D-T neutron spectra.

1- $r_2 >> 1$; 2- $r_2 = 0.2$ (r_2- radius of hot target nucleus).

Kaliski, S., and B. Kaminski. Numerical solutions to plane boundary-value problems of the laser heating of a two-temperature plasma with generation of nuclear fusion energy. Proc. Vibrat. Probl. Pol. Acad. Sci., v. 15, no. 2, 1974, 91-103. (Translation)

Laser heating of a two-temperature plasma is numerically modelled, taking into account nuclear fusion energy. Investigations are conducted on a one-dimensional steady-state model with completely ionized ideal gas having different ion and electron temperatures, where ion and

electron viscosities can be neglected and ion thermal conductivity is low. Electron thermal conductivity and relaxation time of ion and electron temperatures are accounted for. The boundary problem is fixed by assigning an energy flux and pressure at the plasma boundary. The method of radiation absorption by plasma is not considered; only plasma bremsstrahlung is taken into account.

The problem is solved numerically by the method of finite differences according to a trial-run iteration method. Profiles are determined for pressure, temperature, density and velocity of the plasma, and effects of nuclear fusion energy on their forms are studied. Thermal and shock waves are segregated. The limiting transition is plotted for the case of a one-temperature plasma.

Kaliski, S. An appraisal of the average velocity of penetration of a thermal wave into a plasma, using the model of continuous ablation of the outer layer. Bull. Acad. Polon. Sci., Ser. Sci. Techn., no. 7-8, 1974, 59[679]-63[683].

A formula is developed for estimating the average penetration velocity of laser-produced thermal waves into a D-T plasma ball, based on a model of continuous ablation of the outer layer. An example is given for calculating the average velocity of thermal wave penetration, using the developed formula. The author treats the derived formula as a starting point in the development of simplified averaged equations for laser compression of a D-T plasma for the purpose of thermonuclear microfusion.

Kaliski, S. Transformation of concentric shock compression of a nonhomogeneous medium into isentropic compression. Bull. Acad. Polon. Sci., Ser. Sci. Techn., no. 7-8, 1974, 337[569]-345[577].

The problem of transforming a concentric shock compression of a plasma into a quasi-isentropic one by the method of preselected nonhomogenous density profile is solved, using a system of approximate averaged equations. The solution is quantitatively analyzed for the case of a constant external pressure pulse. A general solution is also obtained for the case of a preselected variable external pressure pulse and nonhomogeneous density profile. It is pointed out that the introduction of a preselected nonhomogeneity of the medium may result in a considerable enhancement of compression effects for the same energy of external pressure pulse.

Kaliski, S. A concentric conduction-type thermal wave moving in a plasma at a constant speed. Bull. Acad. Polon. Sci., Ser. Sci. Techn., no. 7-8, 1974, 53[673]-58[678].

The profile of a laser pulse necessary to produce concentric and eccentric thermal waves propagating in a plasma at a constant velocity was determined, for various propagation symmetries and plasma models. These solutions enable the construction of simplified systems of averaged equations for laser heating of plasma, taking into account the structures of thermal and shock waves.

Kaliski, S. An approximate analysis of the problem of subsonic thermal waves in a perfect gas, and some of its characteristics. Bull. Acad. Polon. Sci., Ser. Sci. Techn., no. 7-8, 1974, 347[579]-355[587].

Characteristics of a particular solution for subsonic thermal waves in an ideal gas (Kaliski, 1973) were studied. A general as well as an approximate solution for the model of continuous ablation and rejection of the outer layer of the plasma ball ($c \ll D$) are given. The author notes that, in spite of a considerable simplification of the problem, analytical evaluations for a number of cases may be useful for developing simplified averaged equations which would account for the structure of the shock wave.

Romanov, G. S., L. K. Stanchits, and F. N. Borovik. Coefficients of light absorption in plasma. ZhPS, v. 21, no. 3, 1974, 424-428.

This article examines the effect of a non-ideal plasma on calculation of absorption coefficient and mean free path of radiation. This problem was studied previously by Nikiforov and Uvarov (Coefficients of light absorption in plasma, Inst. prikladnoy matematiki, AN SSSR. Preprint, Moskva, 1969), where a method is suggested for taking into account the Coulomb interaction between ions and free electrons. The cited work obtained an approximate solution of the Thomas-Fermi equation for a nondegenerated plasma of low density and high temperature.

The present authors repeat the exercise but with a rigorous solution to the Thomas-Fermi equation; this allows evaluation of the case in which interaction is relatively large. Theoretical results are given in tabulated form. It is shown that effects of Coulomb interaction and degeneration of electrons become significant for densities on the order of $10^{23}/cm^3$ and electron temperatures < 10 ev.

Fisher, V. I. Effect of losses on the development of an electron avalanche under optical breakdown. ZhTF, no. 8, 1974, 1682-1886.

This article examines the processes taking place in the focal region as a result of increasing ionization level from initiation to breakdown, during laser breakdown of a gas. The author shows that avalanche ionization, taking into account elastic and diffusion losses, explains the results of experimental studies on the dependence of threshold optical breakdown of inert gases on pressures and characteristic dimensions of the focal region.

At sufficiently high pressures, threshold is determined only by elastic losses and does not depend on diffusion length Λ. For this, the pressure required is for example $p > 100$ atm in helium, or $p > 1000$ atm in argon. The role of diffusion losses increases with drop in pressure. At pressures $p < 1$ atm, the threshold is determined mainly by diffusion losses. With comparatively higher Λ, the threshold for argon in the range of 1-10 atm is determined by ionization velocity. At both low Λ and low pressures, electron avalanche cannot occur, in which case the threshold breakdown may be the result of multiphoton ionization.

Fisher, V. I. Laser breakdown of gases in a permanent magnetic field. ZhETF, v. 67, no. 2, 1974, [illegible]1-606.

A rigorous analysis is made of laser breakdown of gas in a constant magnetic field, based on the development of an electron avalanche. It is noted that at a radiation frequency $\omega << (I-I^*)/\hbar$ (where I and I^* are ionization and excitation potential of atoms, respectively), excitation of atoms inhibits the avalanche development, while at $\omega < (I-I^*)/\hbar$, the effect of excitation state depends upon the intensity of radiation. Diffusion of

electrons from the focal region slows down avalanche development, but a magnetic field parallel to the radiation flux inhibits diffusion in the transverse direction, thus facilitating optical breakdown of the gas.

The author offers a simple model of optical breakdown, in which it is assumed that radiation intensity $q(r, \ell)$ changes very little during the time of avalanche and equals q_o inside a cylinder of radius r_o and height $2\ell_o$, becoming zero outside this volume. An equation is derived for determining the frequency of avalanche development, which enables one to calculate optical breakdown threshold of a gas for any values of experimentally measured parameters. It is shown that at magnetic field intensities $H \geq 10^2$ koe, radiation intensity for breakdown threshold decreases by a small factor at pressures $p = 1$ atm, and by more than 10 times at $p = 0.1$ atm. Fig. 1 shows

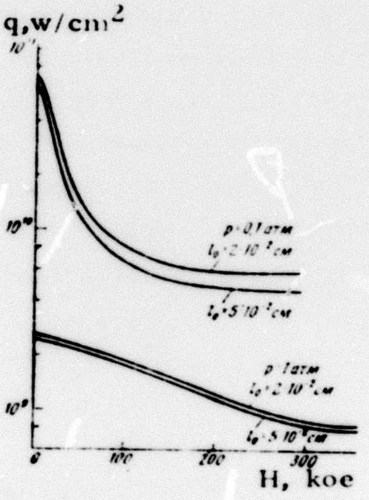

Fig. 1. Breakdown threshold of helium by CO_2 laser radiation in a magnetic field. Avalanche development time $\tau = 10^{-7}$ sec; $r_o = 5 \times 10^{-3}$ cm.

the calculated values of the threshold optical breakdown of helium by a CO_2 laser, as a function of applied magnetic field at pressures of 1 and 0.1 atm.

Litvak, A. G., and V. A. Mironov. Stimulated scattering and decay interaction of waves in a semiconfined plasma. IVUZ Radiofiz, no. 9, 1974, 1281-1286.

Parametric instability is discussed of potential and nonpotential surface waves, generated as a result of intensive e-m waves falling on a nontransparent isothermal plasma with sharp boundaries. The problem is attacked with the method suggested earlier by the authors (ZhETF, 60, 1972, 1702), which is based on the fact that if two waves of near frequencies ω_1 and ω_2 propagate in a plasma, then a low-frequency electric field with difference frequency $\Omega = \omega_1 - \omega_2$ is generated, which interacts with plasma particles. The efficiency of this interaction is determined by the work done by the pulsation field over the particles. A semi-confined plasma ($x > 0$) bounded by a vacuum of $x < 0$ is considered, and an equation is derived for the work done by the electromagnetic field over the plasma, allowing for inhomogeneities in the field. Based on the equations obtained, processes are discussed of stimulated scattering of incident waves on the surface of an isothermal plasma. The increment of instability is determined and threshold fields are estimated.

Analysis of the obtained relationships shows that parametric instability in a confined plasma with sharp boundaries is characterized by significantly high values of threshold fields, as compared to similar processes near the region of plasma resonance in a plasma with diffused boundaries. This is connected with the fact that surface waves have significantly higher linear Landau attenuation than internal waves. Furthermore, the cited effects lead to instability of the homogeneous skin layer of incident waves, and to subsequent breakup of the skin layer into sets of narrow regions (filamentary channels), as a result of the displacement of plasma from loops of increasing stationary waves. Hence these effects can play an important role in nonlinear interaction of an intensive e-m radiation with plasma.

Rykalin, N. N., A. A. Uglov, and M. M. Nizametdinov. Laser breakdown of a gas at low flow densities and high pressures. DAN SSSR, v. 218, no. 2, 1974, 330-331.

Effects of laser breakdown of nitrogen were studied at flux densities of 10^6--10^7 w/cm^2 and nitrogen pressures of 90-120 atm. Experiments were conducted with a free-running neodymium laser on a series of metal targets. A laser beam with spike duration = 6 x 10^{-4} sec, energy up to 10 joule and focal area = 10^{-2} cm^2 was introduced through the window in a high pressure chamber and was focused on molybdenum plates and stainless steel of 1-2 mm thickness by a lens of f = 15 cm, located inside the chamber. High-speed photographs were taken of interaction processes (Fig. 1). Average radiation flux density was about one half the threshold for nitrogen breakdown.

Fig. 1. Photos of laser radiation interaction zone on stainless steel. Time interval between each photo = 60 μsec. P = 120 atm, E = 10 joules; 1- metal; 2- plasma.

The character of the radiation interaction zone on the target was a function of ambient gas pressure. At ~ 90-120 atm, the material surface was almost completely shielded from the beam. Dropping the pressure below 90 atm allowed some fusion at the center of the interaction zone; craters appeared at still lower pressures. At pressures below 10 atm holes were punched through the specimen plates.

It was seen from photographs that effective shielding of the interaction zone at 90 atm begins 30-50 μ sec after the pulse interaction with the target. The average expansion velocity of the shielding plasma cloud counter to the beam direction equalled about 10 m/sec. The authors suggest that the mechanism of gas breakdown leading to the shielding of interaction zone at relatively low flux density may be connected with the development of a gas ionization avalanche, when the source of electrons in the breakdown zone is thermionic emission from the heated metal target surface. Calculations show that the number of electrons released during $\sim$ 10-50 μsec by thermionic emission from the target surface equals 10^{13}-10^{14} in the focus zone, which is the conventional criterion for gas breakdown.

Volyak, T. B., S. D. Kaytmazov, A. M. Prokhorov, and Ye. I. Shklovskiy. Increasing the absorption of laser radiation by a plasma near the target in a strong magnetic field. DAN SSSR, v. 218, no. 1, 1974, 81-83.

The effect of a magnetic field on the intensity of x-radiation from a laser plasma was experimentally studied. An ebonite rather than metallic target was used so as to avoid field absorption effects near the target. Neodymium laser radiation at $\lambda = 1.06$ μ was focused on the target surface, which was placed in the evacuated operating space of a pulsed magnetic device (not shown). Laser pulse duration was 50 nsec at an energy of 5 joules; duration of the field in the magnetic device was 150 μsec and its maximum value was reached in 70-80 μ sec after triggering by impact of the laser pulse on target. X-radiation of the plasma formed was segregated by beryllium foils (70 μm in the 1st channel and 190 μm in the 2nd channel). The peak value of the magnetic field was synchronized with the time of laser pulse arrival within an accuracy of 10%.

Experimental results are shown in the histograms of Fig. 1. It is seen that the field strongly affects the x-ray generation

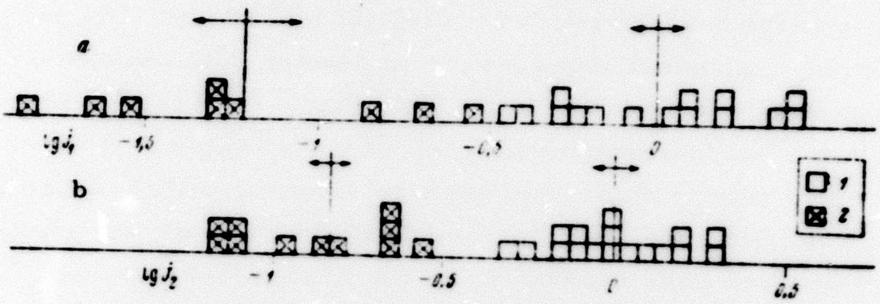

Fig. 1. Effect of magnetic field on x-ray intensity passing through beryllium foils of thickness (a) 70 μm and (b) 190 μm. Log intensities in relative units are shown along the abscissa. Arrows indicate the rms error in average values of intensity. 1 - H = O, 2 - H = 200 koe.

from an ebonite plasma, decreasing its intensity by an average 10 times. The intensity of x-radiation transmitted by the foils was found to decrease by 15 and 7 times respectively. This is due to the increased absorption of laser radiation energy by the plasma flare near the target, thereby significantly reducing the laser energy incident on the target. A comparison of the histograms also shows that the decrease of x-ray intensity in the magnetic field is accompanied by an increase in radiation hardness. This may be explained by different mechanisms, e.g. lowering of the electron thermal conductivity of the plasma due to the field near the target, and decrease in the heated mass of the target material.

A comparison of crater sizes on the impact zone also shows a pronounced reduction in crater size when a field is applied, e.g. by a factor of 3 for H = 200 koe.

Aliyev, Yu. M., S. Vukovich, O. M. Gradov, and A. Yu. Kiriy. Generation of harmonics during scattering of intense electromagnetic waves by surface oscillation fluctuations. ZhETF, v. 68, no. 1, 1975, 85-94.

Spectral correlation functions are obtained for electromagnetic fields of surface oscillations in a stable plasma under the action of intense electromagnetic waves. No condition is put on the level of the incident wave field intensity. The presence of strong e-m waves can cause anisotropy in the correlation function of HF surface wave fields, and the spectral correlation function for a particular direction of surface wave propagation can become zero.

Expressions are obtained for the correlation function of LF surface waves, the spectrum of which is determined by external wave fields. Spectral radiation flux from plasma will be detected, occurring as a result of noncoherent scattering of strong e-m waves by quasistatic surface oscillations, whose wavelengths $1/k_{11}$ are significantly shorter than those of external waves ω_o/c. Correlation functions and spectral radiation flux are found significantly nonlinear as a function of external wave amplitude.

It is shown that during linear interaction of polarized HF e-m waves with surface fluctuations, harmonics of the external field frequency ω_o occur in the spectrum of scattered radiations. At relatively low harmonics $n < (\omega_o/k_{11}c)^{-1}$, scattered radiations are localized near the plasma boundary, while for higher values of harmonics, $n > (\omega_o/k_{11}c)^{-1}$, they are radiated from the plasma.

Burunov, Ye. A., G. M. Malyshev, G. T. Razdobarin, V. V. Semenov, and I. P. Folomkin. Stimulated scattering of laser radiation in plasma. ZhETF, v. 68, no. 1, 1975, 111-114.

In the present work, it was experimentally observed that during scattering of laser radiation in a plasma, the scattered radiation power

for the ion spectral component is significantly higher than the level of corresponding scattering by thermal fluctuations. Experiments were conducted with a 30 Mw ruby laser, with radiation focused in a plasma at a spot diameter of 0. 3 mm. Wave vectors of incident and scattered radiation were perpendicular to each other.

Scattered radiation was observed from the plasma flare at successive intervals from one microsecond to tens of microseconds after breakdown. Scattering bore a collective character ($\alpha = 1/kr_D > 1$, where r_D = Debye radius for electrons, depending on concentration and temperature). Values of electron density and temperature in the plasma flare were determined according to collective dispersion spectra for different moments of time (Fig. 1). Based on these data, values of signals scattered by thermal fluctuations in the ion spectral component were calculated and plotted as a function of time (Fig. 2, curve 1).

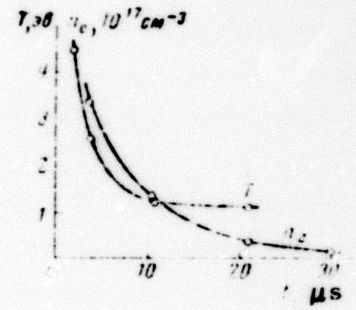

Fig. 1. Time dependences of concentration n_e and temperature T.

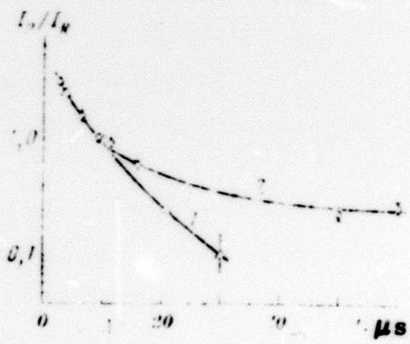

Fig. 2. Intensity of scattered radiation as a function of time.

1 - calculated curve for scattering by thermal fluctuations; 2 - experimental curve.

Curve 2 in Fig. 2 shows the experimental values of scattered signals in plasma for ion components. It is seen that these scattered signals in plasma coincide well with those of calculated thermal fluctuations up to the first 10 μsec, after which they gradually increase and at 30 μsec, they exceed the scattering due to thermal fluctuations by more than 3 times. This increase in signal scattering in the plasma is explained as a function of threshold excitation conditions of parametric instability in the plasma under e-m irradiation.

Bakeyev, A. A., Yu. M. Vas'kovskiy, N. N. Vorob'yeva, L. I. Nikolashina, V. K. Orlov, R. Ye. Rovinskiy, A. K. Sedov, and L. P. Shirokova. Experimental study of the interaction of laser radiation with an argon plasma. Kvantovaya elektronika, no. 1, 1975, 73-77.

A plasmatron-generated argon plasma with initial temperature of 9500° K and electron density $= 10^{16}$ cm^{-3} was exposed to a laser beam with a diameter of 1 cm and Gaussian energy distribution.

The resulting disturbance of the plasma was observed at a power density of the order of 10^{7} w/cm^{2}. The development of the disturbance zone in the plasma is illustrated in Fig. 1. The brightness temperature changed only insignificantly over the duration of the laser pulse (Fig. 2). The velocity of disturbance propagation parallel and perpendicular to the laser beam direction was determined to be: 5 km/sec and 1 km/sec respectively at the initial moment; 200 m/sec and 120 m/sec after 25-30 μsec (see Fig. 3). The plasma temperature increased to $19,000 \pm 1000^{\circ}$ K.

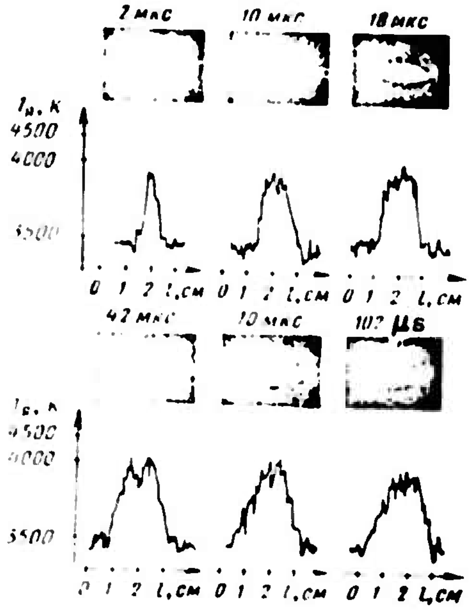

Fig. 1. Distributions of brightness temperature along the axis of the disturbance zone at different moments of interaction. $q_0 = 10^7$ w/cm^2, $\lambda = 0.63\mu$.

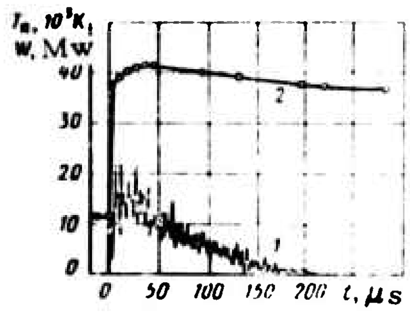

Fig. 2. Time variation of laser pulse (1) and maximum brightness temperature (2) in the disturbance zone.

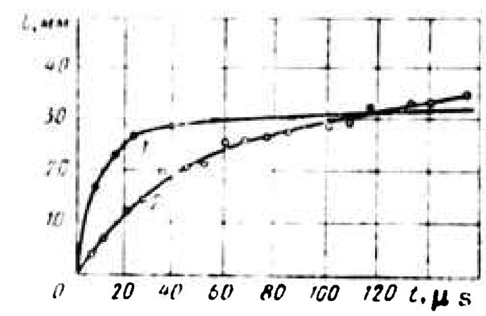

Fig. 3. Change in size of the disturbance zone along (1) and across (2) laser beam.

The test results thus agree well with the threshold power density of 10^7 w/cm^2, which was estimated on the assumption that all the laser energy absorbed by a unit volume of a weakly ionized plasma goes towards increasing its internal energy. Results also showed that the measured values of velocity of disturbance propagation in the initial stage of exposure are consistent with the theory of optical detonation; following

this initial period on the order of 10 μs, a "slow-burning" mode remained in effect for the duration of the pulse. Energy loss to the plasma was less than 3%, which was the measurement threshold.

SOURCE ABBREVIATIONS

AiT	-	Avtomatika i telemekhanika
APP	-	Acta physica polonica
DAN ArmSSR	-	Akademiya nauk Armyanskoy SSR. Doklady
DAN AzSSR	-	Akademiya nauk Azerbaydzhanskoy SSR. Doklady
DAN BSSR	-	Akademiya nauk Belorusskoy SSR. Doklady
DAN SSSR	-	Akademiya nauk SSSR. Doklady
DAN TadSSR	-	Akademiya nauk Tadzhikskoy SSR. Doklady
DAN UkrSSR	-	Akademiya nauk Ukrainskoy SSR. Dopovidi
DAN UzbSSR	-	Akademiya nauk Uzbekskoy SSR. Doklady
DBAN	-	Bulgarska akademiya na naukite. Doklady
EOM	-	Elektronnaya obrabotka materialov
FAiO	-	Akademiya nauk SSSR. Izvestiya. Fizika atmosfery i okeana
FGiV	-	Fizika goreniya i vzryva
FiKhOM	-	Fizika i khimiya obrabotka materialov
F-KhMM	-	Fiziko-khimicheskaya mekhanika materialov
FMiM	-	Fizika metallov i metallovedeniye
FTP	-	Fizika i tekhnika poluprovodnikov
FTT	-	Fizika tverdogo tela
FZh	-	Fiziologicheskiy zhurnal
GiA	-	Geomagnetizm i aeronomiya
GiK	-	Geodeziya i kartografiya
IAN Arm	-	Akademiya nauk Armyanskoy SSR. Izvestiya. Fizika
IAN Az	-	Akademiya nauk Azerbaydzhanskoy SSR. Izvestiya. Seriya fiziko-tekhnicheskikh i matematicheskikh nauk

IAN B	-	Akademiya nauk Belorusskoy SSR. Izvestiya. Seriya fiziko-matematicheskikh nauk
IAN Biol	-	Akademiya nauk SSSR. Izvestiya. Seriya biologicheskaya
IAN Energ	-	Akademiya nauk SSSR. Izvestiya. Energetika i transport
IAN Est	-	Akademiya nauk Estonskoy SSR. Izvestiya. Fizika matematika
IAN Fiz	-	Akademiya nauk SSSR. Izvestiya. Seriya fizicheskaya
IAN Fizika zemli	-	Akademiya nauk SSSR. Izvestiya. Fizika zemli
IAN Kh	-	Akademiya nauk SSSR. Izvestiya. Seriya khimicheskaya
IAN Lat	-	Akademiya nauk Latviyskoy SSR. Izvestiya
IAN Met	-	Akademiya nauk SSSR. Izvestiya. Metally
IAN Mold	-	Akademiya nauk Moldavskoy SSR. Izvestiya. Seriya fiziko-tekhnicheskikh i matematicheskikh nauk
IAN SO SSSR	-	Akademiya nauk SSSR. Sibirskoye otdeleniye. Izvestiya
IAN Tadzh	-	Akademiya nauk Tadzhiksoy SSR. Izvestiya. Otdeleniye fiziko-matematicheskikh i geologo-khimicheskikh nauk
IAN TK	-	Akademiya nauk SSSR. Izvestiya. Tekhnicheskaya kibernetika
IAN Turk	-	Akademiya nauk Turkmenskoy SSR. Izvestiya. Seriya fiziko-tekhnicheskikh, khimicheskikh, i geologicheskikh nauk
IAN Uzb	-	Akademiya nauk Uzbekskoy SSR. Izvestiya. Seriya fiziko-matematicheskikh nauk
IBAN	-	Bulgarska akademiya na naukite. Fizicheski institut. Izvestiya na fizicheskaya institut s ANEB
I-FZh	-	Inzhenerno-fizicheskiy zhurnal

IiR	-	Izobretatel' i ratsionalizator
ILEI	-	Leningradskiy elektrotekhnicheskiy institut. Izvestiya
IT	-	Izmeritel'naya tekhnika
IVUZ Avia	-	Izvestiya vysshikh uchebnykh zavedeniy. Aviatsionnaya tekhnika
IVUZ Cher	-	Izvestiya vysshikh uchebnykh zavedeniy. Chernaya metallurgiya
IVUZ Energ	-	Izvestiya vysshikh uchebnykh zavedeniy. Energetika
IVUZ Fiz	-	Izvestiya vysshikh uchebnykh zavedeniy. Fizika
IVUZ Geod	-	Izvestiya vysshikh uchebnykh zavedeniy. Geodeziya i aerofotos"yemka
IVUZ Geol	-	Izvestiya vysshikh uchebnykh zavedeniy. Geologiya i razvedka
IVUZ Gorn	-	Izvestiya vysshikh uchebnykh zavedeniy. Gornyy zhurnal
IVUZ Mash	-	Izvestiya vysshikh uchebnykh zavedeniy. Mashinostroyeniye
IVUZ Priboro	-	Izvestiya vysshikh uchebnykh zavedeniy. Priborostroyeniye
IVUZ Radioelektr	-	Izvestiya vysshikh uchebnykh zavedeniy. Radioelektronika
IVUZ Radiofiz	-	Izvestiya vysshikh uchebnykh zavedeniy. Radiofizika
IVUZ Stroi	-	Izvestiya vysshikh uchebnykh zavedeniy. Stroitel'stvo i arkhitektura
KhVE	-	Khimiya vysokikh energiy
KiK	-	Kinetika i kataliz
KL	-	Knizhnaya letopis'
Kristall	-	Kristallografiya
KSpF	-	Kratkiye soobshcheniya po fizike

LZhS	-	Letopis' zhurnal'nykh statey
MiTOM	-	Metallovedeniye i termicheskaya obrabotka materialov
MP	-	Mekhanika polimerov
MTT	-	Akademiya nauk SSSR. Izvestiya. Mekhanika tverdogo tela
MZhiG	-	Akademiya nauk SSSR. Izvestiya. Mekhanika zhidkosti i gaza
NK	-	Novyye knigi
NM	-	Akademiya nauk SSSR. Izvestiya. Neorganicheskiye materialy
NTO SSSR	-	Nauchno-tekhnicheskiye obshchestva SSSR
OiS	-	Optika i spektroskopiya
OMP	-	Optiko-mekhanicheskaya promyshlennost'
Otkr izobr	-	Otkrytiya, izobreteniya, promyshlennyye obraztsy, tovarnyye znaki
PF	-	Postepy fizyki
Phys abs	-	Physics abstracts
PM	-	Prikladnaya mekhanika
PMM	-	Prikladnaya matematika i mekhanika
PSS	-	Physica status solidi
PSU	-	Pribory i sistemy upravleniya
PTE	-	Pribory i tekhnika eksperimenta
Radiotekh	-	Radiotekhnika
RiE	-	Radiotekhnika i elektronika
RZhAvtom	-	Referativnyy zhurnal. Avtomatika, telemekhanika i vychislitel'naya tekhnika
RZhElektr	-	Referativnyy zhurnal. Elektronika i yeye primeneniye

RZhF	-	Referativnyy zhurnal. Fizika
RZhFoto	-	Referativnyy zhurnal. Fotokinotekhnika
RZhGeod	-	Referativnyy zhurnal. Geodeziya i aeros"-yemka
RZhGeofiz	-	Referativnyy zhurnal. Geofizika
RZhInf	-	Referativnyy zhurnal. Informatics
RZhKh	-	Referativnyy zhurnal. Khimiya
RZhMekh	-	Referativnyy zhurnal. Mekhanika
RZhMetrolog	-	Referativnyy zhurnal. Metrologiya i izmeritel'naya tekhnika
RZhRadiot	-	Referativnyy zhurnal. Radiotekhnika
SovSciRev	-	Soviet science review
TiEKh	-	Teoreticheskaya i eksperimental'naya khimiya
TKiT	-	Tekhnika kino i televideniya
TMF	-	Teoreticheskaya i matematicheskaya fizika
TVT	-	Teplofizika vysokikh temperatur
UFN	-	Uspekhi fizicheskikh nauk
UFZh	-	Ukrainskiy fizicheskiy zhurnal
UMS	-	Ustalost' metallov i splavov
UNF	-	Uspekhi nauchnoy fotografii
VAN	-	Akademiya nauk SSSR. Vestnik
VAN BSSR	-	Akademiya nauk Belorusskoy SSR. Vestnik
VAN KazSSR	-	Akademiya nauk Kazakhskoy SSR. Vestnik
VBU	-	Belorusskiy universitet. Vestnik
VNDKh SSSR	-	VNDKh SSSR. Informatsionnyy byulleten'
VLU	-	Leningradskiy universitet. Vestnik. Fizika, khimiya
VMU	-	Moskovskiy universitet. Vestnik. Seriya fizika, astronomiya

ZhETF	-	Zhurnal eksperimental'noy i teoreticheskoy fiziki
ZhETF P	-	Pis'ma v Zhurnal eksperimental'noy i teoreticheskoy fiziki
ZhFKh	-	Zhurnal fizicheskoy khimii
ZhNiPFiK	-	Zhurnal nauchnoy i prikladnoy fotografii i kinematografii
ZhNKh	-	Zhurnal neorganicheskoy khimii
ZhPK	-	Zhurnal prikladnoy khimii
ZhPMTF	-	Zhurnal prikladnoy mekhaniki i tekhnicheskoy fiziki
ZhPS	-	Zhurnal prikladnoy spektroskopii
ZhTF	-	Zhurnal tekhnicheskoy fiziki
ZhVMMF	-	Zhurnal vychislitel'noy matematiki i matematicheskoy fiziki
ZL	-	Zavodskaya laboratoriya